Cell Biological Studies on Adipocyte-Macrophage Communication

Master thesis

of

Annabell Witzke

Table of content

Zusammenfassung

Adipositas und damit assoziierte Krankheitsbilder haben sich zu einem erheblichen Gesundheitsrisiko entwickelt. Auf Grund der Einwanderung von Makrophagen in das Fettgewebe, kommt es dort zu einer chronischen Entzündung. Suganami, et al. (1) konnten zeigen, dass ein parakriner Kommunikationsweg zwischen Adipozyten und Makrophagen besteht, welcher die, in einer in vitro Co-Kultur beobachteten, Effekte verstärkt. Darüber hinaus wurden freie Fettsäuren und der Tumornekrosefaktor α (TNFα) als zentrale Bestandteile des Teufelskreises identifiziert.

Das Ziel dieser Masterarbeit war es, die Zell-Zell-Kummunikation in einem in vitro Co-Kultursystem aus 3T3-L1 Adipozyten und RAW264.7 Makrophagen zu untersuchen. Das entsprechende Co-Kultursystem wurde für mehr-Kapazität-Formate etabliert und entsprechend erweitert, um die Untersuchung und Quantifizierung von Proteinen zu ermöglichen. Ein Schwerpunkt der Arbeit lag dabei auf der Proteom-weiten Erfassung der Zell-Zell-Kommunikation mittels Massenspektrometrie. Des Weiteren erwiesen sich 24 Stunden als optimale Inkubationszeit der Co-Kultur, um massenspektrometrisch Veränderungen zu quantifizieren. Mit Hilfe von biomolekularen Indikatoren, wie z.B. Adiponectin, TNFα, MCP-1, IL-6, Cox-2 und freien Fettsäuren, konnten Veränderungen in der RNS-Expression und auf metabolischer Ebene nachgewiesen werden. Außerdem wurde die Phosphorylierung von dem inflammatorischen Schlüsselmolekül JNK und seiner Effektorproteine (cJun und IRS-1) mittels Western Blot näher betrachtet.

Basierend auf den durchgeführten Experimenten, konnte gezeigt werden, das die Co-Kultur von Adipozyten und Makrophagen grundlegende Auswirkungen auf die RNS Expression und das Proteom hat. In einem elektrophorese-basierten Ansatz wurden im Durchschnitt 235 Proteine pro Gelstück ermittelt, darunter LPL, Perilipin, Cyp2f2 und TLR2. Des Weiteren wurden zahlreiche metabolische Stoffwechselwege, wie z.B. oxidative Phosphorylierung und Pentose-Phosphatweg indentifiziert. Weiterhin war es möglich, die Co-Kultur mit der Methode „stable isotope labeling with amino acids in cell culture“ (SILAC) zu kombinieren. Auf diese Weise wurden 3 Enzyme der Glykolyse ermittelt, welche in co-kultivierten RAW264.7 Zellen hochreguliert waren.

Summary

Obesity and its co-morbidities have developed into a major health threat. Due to the infiltration of macrophages, obese adipose tissue is characterized by chronic low-grade inflammation. Suganami, et al. (1) suggested the existence of a paracrine loop between adipocytes and macrophages, which aggravates coculture-induced changes. Moreover, free fatty acids and TNFα were identified as major components of this vicious cycle.

The aim of this master thesis was to use an in vitro coculture system comprising 3T3-L1 adipocytes and RAW264.7 macrophages in order to study the cell-cell communication. This coculture system was established successfully for multiple well formats and up-scaled for protein harvest. A particular emphasis lay on enabling a proteome-wide detection of intra-cellular communication by mass spectrometry. Moreover, 24 hours of incubation proved to be optimal for MS analysis. Furthermore, biomarkers including Adiponectin, TNFα, MCP-1, IL-6, Cox-2 and FFAs were used to study the adipocyte-macrophage communication on the RNA expression and metabolic level. In Addition, the phosphorylation state of JNK, an inflammatory key molecule, and its target molecules including cJUN and IRS-1 were studied by western blotting.

Based on the performed experiments, it was proven that coculture of adipocytes and macrophages resulted in major changes concerning RNA expression and protein levels. A set of biomarkers was established to study coculture-induced effects. Furthermore, phosphorylation of JNK and cJun, was induced under cocultural conditions. In a SDS-Page-based approach on average 235 proteins were identified per slice. Several important proteins including LPL, perilipin, Cypf2f2 and TLR2 and various metabolic pathways (TCA cycle, pentose phosphate pathways, oxidative phosphorylation) were identified. Coculture experiments in an up-scaled system were successfully combined with stable isotope labeling with amino acids in cell culture (SILAC). Thereby, three glycolytic enzymes were found up-regulated in RAW264.7 macrophages after 8 hours of coculture.

1. Introduction

1.1. Obesity as a growing health problem

Obesity and its co-morbidities as type 2 diabetes, liver steatosis and atherosclerosis (2) are a major problem of modern days. Obesity belongs to a metabolic disease cluster, termed metabolic syndrome (Figure 1). In general the term metabolic syndrome stands for the constellation of visceral fat obesity, insulin resistance, atherogenic dyslipidemia, and hypertension (3-5).

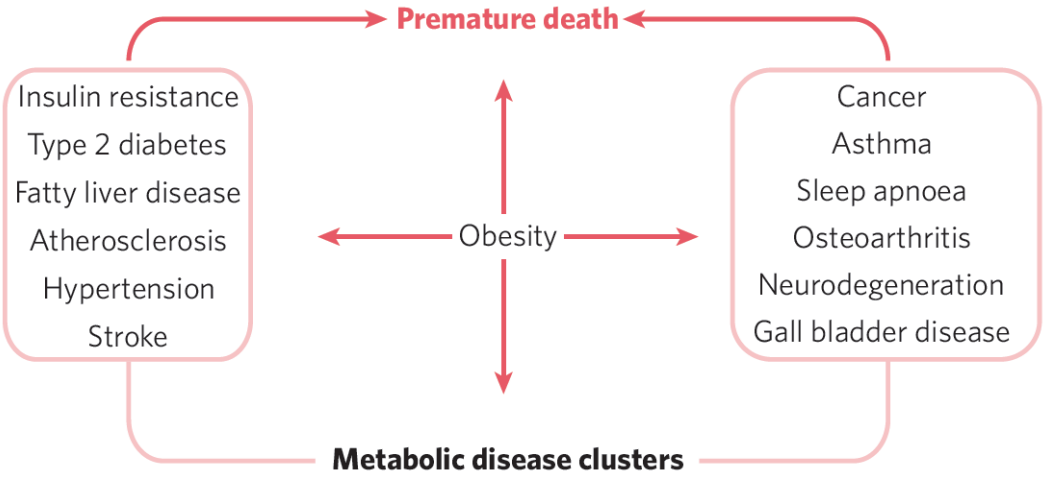

Figure 1: Metabolic disease clusters. Obesity is suggested to increase the risk for various diseases although the linking mechanisms are only poorly understood (5).

As the incidence of obesity is increasing dramatically worldwide, this disease cluster developed to a serious health threat. Not only the total amount of fat, but also the distribution of adipose tissue is very important for the course of obesity. In particular visceral fat depots are considered as main contributors to insulin resistance (6).

In general, obesity, insulin resistance and type 2 diabetes are closely associated with a state of chronic low-grade inflammation (3-5, 7), which can be further characterized by abnormal cytokine production and activation of various inflammatory signaling pathways (8). While a termination program could resolve acute inflammation, chronic inflammation is characterized by persistent stress without termination (9). Therefore chronic inflammation results in functional mal-adaption and in case of obesity in tissue remodeling (10). Moreover, obese adipose tissue is characterized by several dynamic changes that concern the cellular composition and function (Figure 2). Hypertroph

adipocytes induce infiltration of immune cells (3, 5, 11), a process termed adipose tissue remodeling (9). Macrophages can invade adipose tissue and activate inflammatory pathways (12-15).

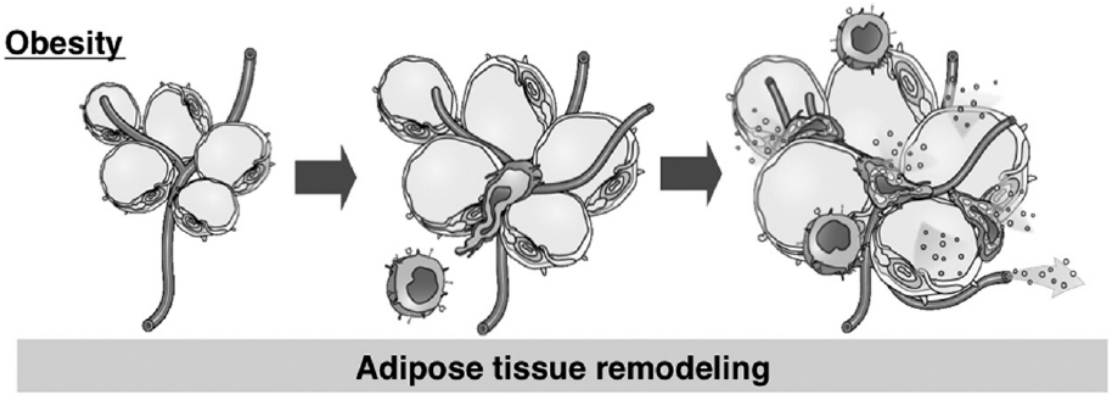

Figure 2: Adipose tissue remodeling (adapted from Suganami and Ogawa (16)).

Markedly increased macrophage infiltration is the main cause for the chronic and low-grade inflammation state of obese adipose tissue (17), which in the end results in a decreased insulin sensitivity of adipocytes (18). This suggests that infiltrated macrophages may play an important role in adipose tissue inflammation and insulin resistance. Recently Suganami, et al. (1) showed, that the paracrine loop, involving saturated fatty acids derived from adipocytes and tumor necrosis factor-α derived from macrophages, aggravates obesity-induced adipose tissue inflammation.

The fat storing tissue is nowadays known as regulator of several processes and source of adipokines (17). Adipokines are bioactive substances secreted by the adipose tissue. An unbalanced production of pro- and anti-inflammatory adipokines, which is the case in obese adipose tissue, can contribute to the development of the metabolic syndrome (3-5). Mohamed-Ali, et al. (19) showed that obesity gives rise to quantitative and qualitative alterations in adipose tissue signaling.

1.2. Insulin resistance and insulin signalling

Several abnormalities are associated with insulin resistance, including a decreased glucose uptake into the skeletal muscle and adipose tissue (20). Insulin resistance is a pathologic state in which metabolic target tissues fail to respond to normal insulin

levels, and is furthermore a key predictor for the development of a variety of metabolic diseases such as type 2 diabetes or the metabolic syndrome (21).

The insulin receptor belongs to the so-called receptor tyrosine kinase family, which possesses an intrinsic tyrosine kinase activity and commonly uses a docking protein for signal mediation. The insulin receptor substrate (IRS) proteins, comprising 6 isoforms, are generally tyrosine phosphorylated due to insulin signalling. IRS-1 gets phosphorylated as result of insulin receptor (IR) signalling and impairs further signalling. IRS-1 itself contains various potential tyrosine and serine/threonine phosphorylation sides. Several molecules and cytokines including TNFα and free fatty acids (FFAs) target this phosphorylation process, in order to mediate an inhibitory phosphorylation of IRS-1 at a serine residue (5). Moreover various IRS-modifying enzymes including c-Jun-N-terminal kinase (JNK) are known to serine-phosphorylate IRS-1 (22), which interrupts the insulin signalling and further blocks insulin action (5). Gual, et al. (23) identified the phosphorylation of serine residues like Ser307 or Ser632, as a major mechanism in negative feedback. Due to phosphorylation, the association of IRS-1 and the insulin receptor is impaired and thus downstream insulin signalling (23, 24). While IRS-1 is phosphorylated at a tyrosine residue to establish insulin signalling, phosphorylation at serine residue terminates the signalling process.

1.3. Adipose tissue remodelling in obesity

In general, adipose tissue comprises lipid-loaden mature adipocytes and stromal cells, which are preadipocytes, endothelial cells, fibroblasts and immune cells. The dynamic changes during adipose tissue remodeling result in an unbalanced production of pro- and anti-inflammatory adipokines (3, 5, 11, 19). The importance of macrophages infiltrating the obese adipose tissue is emphasized by the finding that macrophage infiltration and inflammation-related gene expression precedes the development of insulin resistance in animal models (12, 13).

Recently a paracrine loop between adipocytes and macrophages was identified to aggravate inflammatory changes (1). Moreover secreted factors, including TNFα and FFAs, were identified as the major source of inflammatory changes (Figure 3).

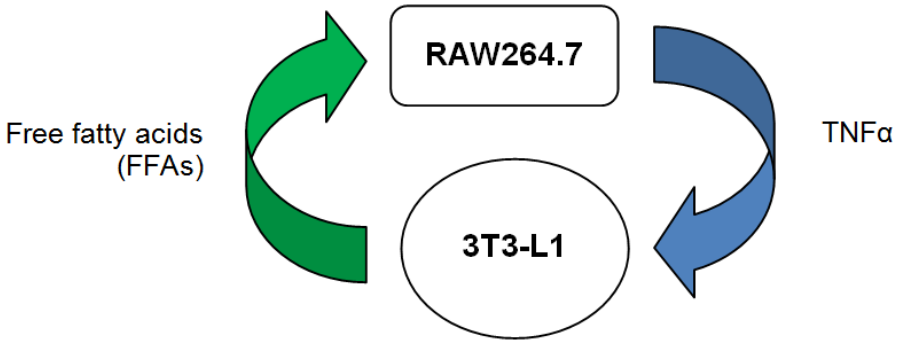

Figure 3: Paracrine loop between adipocytes and macrophages in a coculture system. RAW264.7-deprived TNFα stimulates free fatty acid release by 3T3-L1 adipocytes. RAW264.7 sense free fatty acid and secrete TNFα.

As shown by Weisberg, et al. (12), adipose tissue is usually populated with 5% - 10% macrophages whereas macrophage constitution can increase up to 60% in obese mice. Moreover, the further recruitment of macrophages into the obese adipose tissue is implicated to the increased chemokine production (12).

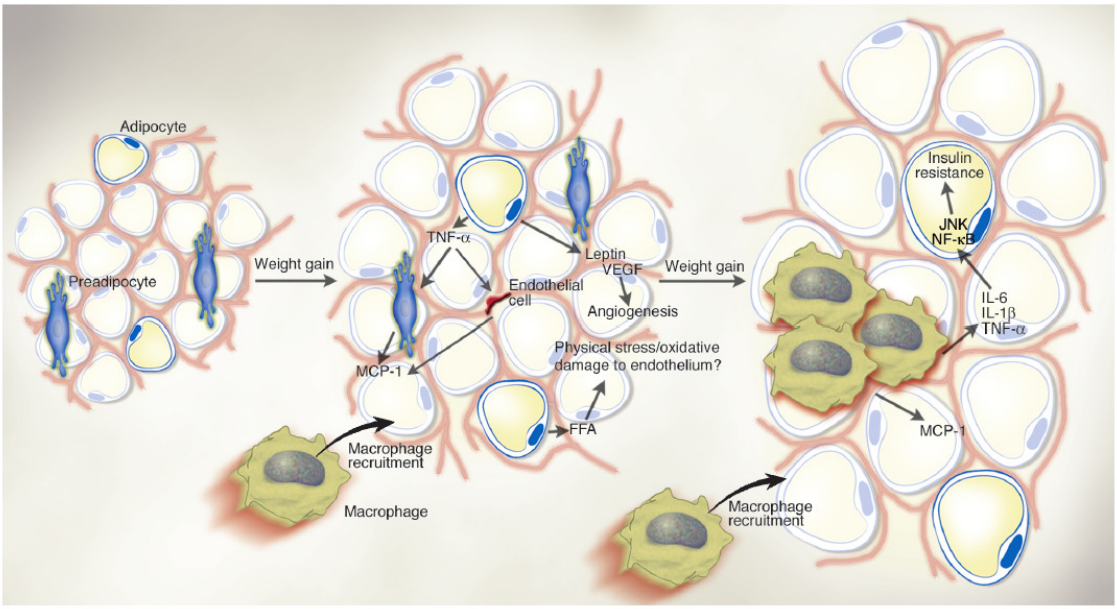

Figure 4: Inflammation of obese adipose tissue. Adipocytes secrete TNFα and MCP-1, which stimulates surrounding cells to produce MCP-1 themselves. Finally, macrophages are recruited into the adipose tissue and mark the starting point of the cell-cell communication. MCP-1, monocyte chemoattractant protein 1; TNFα, tumor necrosis factor α; FFA, free fatty acid; VEGF, vascular endothelial growth factor; JNK, c-Jun amino-terminal kinase; IL-6, Interleukine 6; IL-1β, Interleukin 1β. (25)

The development of adipose tissue remodeling is depicted in Figure 4. At first adipocytes secrete low levels of TNFα, which in turn stimulate preadipocytes to

produce monocyte chemoattractant protein-1 (MCP-1) (13). Concomitantly surrounding cells e.g. endothelial cells begin to secrete MCP-1. As a result, macrophages accumulate in the adipose tissue. Nevertheless the initial stimulus for macrophage recruitment remains unknown. The presence of macrophages in the adipose tissue marks the starting point of a vicious cycle comprising macrophage recruitment, enhanced production of pro-inflammatory markers, and abolishment of adipocyte function (25).

1.3.1. Adiponectin

The 244-amino acids large protein was isolated from 3T3-L1 adipocytes during differentiation and is known under several names including AcrP30, AdipiQ, apM1 and gelatin binding protein. Moreover the anti-inflammatory cytokine is markedly down-regulated in obesity. Thus supplementation of adiponectin provided an effective treatment to reverse insulin resistance in the skeletal muscle and liver of obese mice (26, 27). Furthermore, adiponectin modulates various metabolic processes such as glucose regulation and fatty acid metabolism (28).

1.3.2. Resistin

Resistin was first described in 2001 and is basically a 114-amino acid polypeptide (in mouse) containing a 20-amino acid signal sequence. Resistin expression is induced during adipocyte differentiation but only mature adipocytes secrete resistin as a disulfide-linked dimmer. Moreover expression of resistin is increased by interleukins, lipopolysaccharides (LPS) and in insulin-resistant mice (29-31). Thiazolidinediones (TZD) influence resistin secretion, furthermore insulin action is antagonized by resistin (29). Additionally, resistin was linked to an increased expression of pro-inflammatory markers such as interleukin 1 (IL-1), interleukin 6 (IL-6) and tumor necrosis factor α (TNFα) (32, 33). Recently resistin was suggested as link between inflammation and insulin resistance (8).

1.3.3. Free fatty acids (FFAs)

Free fatty acids (FFAs) are an important energy source generated from triglycerides. Adipose tissue mobilizes triglycerides, particularly under starvation conditions. Moreover, FFAs released during fasting are at least partly responsible for macrophage

recruitment into adipose tissue. It is suggested that during fasting conditions, lipolysis occurs as a regulator of metabolic homeostasis rather than a danger signal (34). However, under over-nutrition conditions increased free fatty acid concentrations activate inflammatory pathways in order to maintain adipose tissue homeostasis such as tissue repair and metabolism regulation. Nevertheless due to excessive or sustained celluar or tissue stress an adaptive response is no longer possible, resulting in prolonged inflammatory response (chronic inflammation) and diseased tissue remodeling (10). In 2002, Boden and Shulman (35) described a physiological and pathophysiological effect of FFAs on glucose homeostasis, which provides further evidence of their metabolic functions. Recently FFAs were identified as a major component of the paracrine loop between adipocytes and macrophages and further as amplifier of the mentioned vicious cycle (1). Furthermore FFAs are natural ligands for the toll-like receptor (TLR) 4 (Figure 5).

1.3.4. Triglycerides (TGs)

Adipose tissue markedly expresses triglyceride synthetic enzymes in order to quickly re-esterify released free fatty acids (FFAs). Inflammatory processes promote lipolysis and increase free fatty acid mobilization by decreasing intracellular fatty acid re-esterification. In general the expression of triglyceride biosynthetic enzymes including acyl-CoA synthetase, glycerol-3-phosphate acyltransferase, 1-acyl-glycerol-3-phosphate acyltransferase, lipin 1, monoacylglyceride acyltransferase and diacylglyceride acyltransferase is decreased (36, 37). Nevertheless the major pathway being accountable for about 90% of triglyceride glycerol synthesis is gluceneogenesis (38). One of the key regulator enzymes is phosphoenolpyruvate carboxykinase (PEPCK) (37). Recently Feingold, et al. (39) showed that PEPCK expression is influenced by inflammation. In inflamed adipose tissue, PEPCK is decreased as a kind of rapid response in order to increase the availability of fatty acids for export. Hence the serum FFA concentration is increased.

1.3.5. Tumor necrosis factor α (TNFα)

Tumor necrosis factor α (TNFα) is synthesized as 26kDa transmembrane pro-hormone, but secreted as a 17kDa soluble molecule (40). It functions as a pro-inflammatory

cytokine which is able to activate several signaling pathways. In cell culture, it is mostly derived from macrophages, while in adipocytes, TNFα is predominantly unsecreted and membrane-bound (12). Studies indicated that TNFα levels are increased in obese adipose tissue (12, 13) and a lack of TNFα function can improve insulin sensitivity and glucose homeostasis at least in obese mouse models. Moreover, TNFα is capable to inhibit the uptake of free fatty acids (FFAs) and to decrease the expression of key enzymes used for lipogenesis (1, 40). Suganami, et al. (41) showed that TNFα/TNF receptor signaling results in the induction of pro-inflammatory cytokine production and adipocyte lipolysis via nuclear factor-κB (NF-κB) signal cascade (Figure 5). Recently TNFα was identified as the component initiating the paracrine loop between adipocytes and macrophages and further as aggravator of the adipocyte-macrophage communication (1). The coculture of 3T3-L1 adipocytes and RAW264.7 macrophages increased TNFα mRNA expression (1).

1.3.6. Monocyte chemoattractant protein 1 (MCP-1)

Kanda, et al. (42) showed that monocyte chemoattractant protein 1 (MCP-1) gene expression is induced in adipose tissue and that MCP-1 plasma concentration is increased in obese mice. Moreover, MCP-1 is required for macrophage recruitment into adipose tissue (43). Transgenetic Mcp-1 expression increases macrophage infiltration, inflammation and insulin resistance in adipose tissue (42, 43). Therefore it seems to be important for pathogenesis of macrophage infiltration into adipose tissue (Figure 4 and Figure 5), insulin resistance and hepatic steatosis (42). In obese adipose tissue MCP-1 is secreted by adipocytes and macrophages (12, 13). Subsequently MCP-1 aggravates adipose tissue inflammation and can induce insulin resistance in skeletal muscle and liver (42-44). Due to its abilities, MCP-1 is suggested to act as an endocrine hormone (43, 44).

1.3.7. Interleukin 6 (IL-6)

Interleukin 6 (IL-6) is a cytokine with both pro- and anti-inflammatory properties. In general it is variably glycosylated, with a size of 22 to 27kDa, and secreted by many cell types, including immune cells, fibroblasts and adipocytes. As a matter of fact, adipose tissue secretes 10% to 35% of the basal circulating IL-6 (45). Production of

IL-6 is stimulated by Interleukin-1β and tumor necrosis factor α (TNFα). Furthermore IL-6 increases the release of free fatty acids from adipose tissue and is correlated with human obesity and insulin resistance. Coculture of 3T3-L1 adipocytes with RAW264.7 macrophages markedly up-regulated Il-6 mRNA expression (1).

1.3.8. Toll-like receptor 4 (TLR4) and NF-κB signaling

The Toll-like receptor 4 (TLR4) belongs to the family of pattern-recognition receptors, which are essential for the recognition of lipopolysaccharides (LPS). Recently it was shown, that TLR4 plays an important role in obesity-related inflammation and lipid metabolism (41). The receptor is expressed in macrophages, where it functions as a sensor for saturated fatty acids (FFAs), which are released from adipocytes and induce chronic inflammatory responses in macrophages (41, 46, 47). FFAs released from adipocytes are naturally occurring ligands for the TLR4 complex and induce an inflammatory response in macrophages (48). Activation of this complex results in the induction of the NF-κB signaling cascade in macrophages (Figure 5, (41)). In summary, TLR4 could provide a link between nutrition, lipids and inflammation (48).

Already in 2007 Suganami and colleagues demonstrated that coculture of 3T3-L1 adipocytes and RAW264.7 macrophages activates NF-κB. Moreover, a pharmacological inhibition of NF-κB strikingly suppressed the observed production of pro-inflammatory cytokines and lipolysis in coculture. Recently phenylmethimazole (C10) was shown to block TLR-mediated activation of inflammatory pathways in 3T3-L1 adipocytes and RAW264.7 macrophages (49).

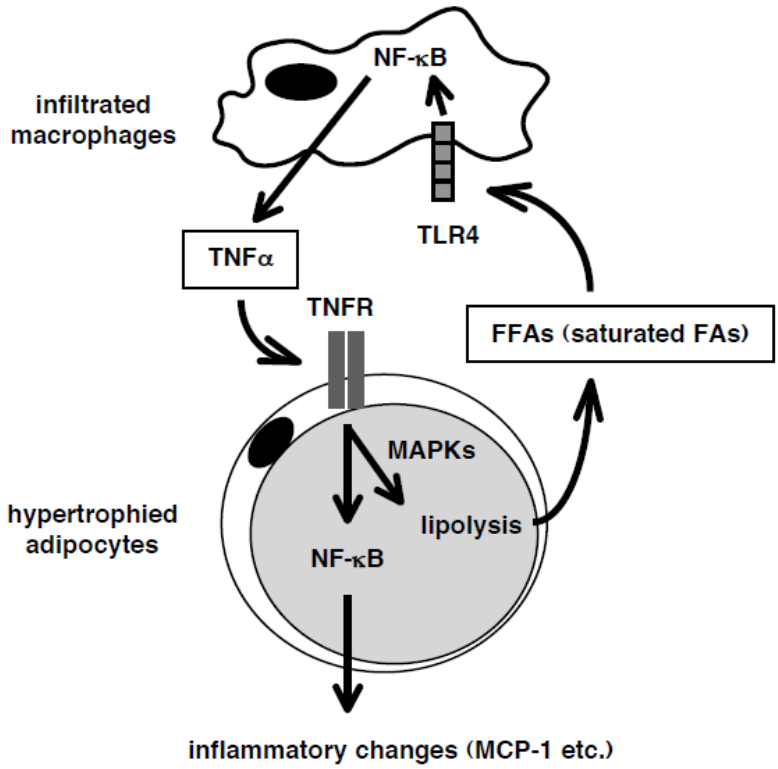

Figure 5: Suggested role of TLR4/NF-κB signaling. Macrophage deprived TNFα, interacts with its receptor (TNFR) and induces inflammatory signaling in adipocytes. FFAs deprived from adipocyte activate TLR4/NF-κB signal cascade in macrophages and induce further TNFα production. TLR4, toll-like receptor 4; TNFα, tumor necrosis factor α; TNF-R, TNFα receptor; MAPKs, mitogen-activated protein kinases, MCP-1, monocyte chemoattractant protein 1. (41)

1.3.9. Macrophage-inducible C-type lectin (Mincle)

The macrophage-inducible C-type lectin, also known as Mincle, Clec4e or Clecsf9 functions as a pathogen sensor for pathogenic fungi and Mycobacterium tuberculosis. Moreover, Mincle is induced in obese adipose tissue macrophages partly through saturated fatty acid/TLR4/NF-*κ*B pathway. Ichioka, et al. (50) suggested a pathophysiologic role in obese adipose tissue inflammation for Mincle. Furthermore, it is suggested to act as pathogen sensor and to induce pro-inflammatory cytokine and chemokine expression (50). Recently Yamasaki, et al. (51) showed, that Mincle serves as receptor for SAP130 (51), a component released from damaged cells, which suggested that Mincle plays a role as sensor of cell death. Due to the fact that in obese adipose tissue (human and mice) dead adipocytes are surrounded by macrophages (11, 52), Mincle might be used to sense adipocyte death, macrophages activation due to FFAs and influence adipose tissue remodeling.

1.4. ER stress and JNK

The adipose tissue is an endocrine organ, capable to secrete biologically active substances, so-called adipokines, which include adiponectin, monocyte chemoattractant protein 1 (MCP-1) and tumor necrosis factor α (TNFα) (3-5, 53-55). Inflammatory changes in the adipose tissue caused by obesity result in a dysregulation of the adipokine production. Furthermore, obese adipose tissue secretes TNFα, interleukin 1 (IL-1) and resistin in order to suppress insulin signalling (29, 53, 56). Characteristically TNFα and MCP-1 are up-regulated in obese adipose tissue, while adiponectin is downregulated (14, 53, 54). Moreover, obesity is associated with endoplasmatic reticulum (ER) stress especially in the adipose tissue and the liver. Hence, ER stress could play an important role in adipose tissue inflammation due to obesity (57). In addition several signaling pathways are activated in obese adipose tissue, resulting in activation of mitogen-acitvated protein kinase (MAPK) and stress-activated c-Jun amino-terminal kinase (JNK) (58).

1.4.1. Endoplasmatic reticulum stress

The endoplasmatic reticulum (ER) is a membrane network and the place where all secretory and membrane proteins are assembled. In general unfolded or misfolded proteins are detected and degraded. Nevertheless, various disturbances lead to the accumulation of unfolded proteins, resulting in cellular stress which in case of the ER activates the unfolded protein response (UPR) mechanism. Obesity was linked to ER stress especially in adipose tissue and the liver (57). Probably, the ER functions as sensor of metabolic stress and translates it into an inflammatory response. Recently it was shown that ER UPR signaling interferes with several inflammatory pathways including JNK- and TLR-mediated signaling (59).

1.4.2. c-Jun amino-terminal kinase (JNK) signalling

The family of stress-activated c-Jun amino-terminal kinases (JNKs) belongs to the mitogen-acitvated protein kinases (MAPK). Of the three isoforms occurring in mammalians, JNK1 and JNK2 are ubiquitously expressed while JNK3 is restricted to the brain, pancreatic islet cells, testes and heart (60). Furthermore, JNKs have been

shown to interfere with insulin signaling (22). Activation of JNK can be a result of inflammatory cytokines, FFAs, ER stress or hyperlipidemia, which are hallmarks of obesity and type 2 diabetes (8, 22, 40, 57, 61). Hirosumi, et al. (58) substantiated a striking increase in JNK activity, which is predominantly provided by JNK1, in both obese adipose and liver tissue. Moreover, they provide the link between increased JNK activation and inhibitory phosphorylation of IRS-1 at Ser307. Phosphorylation of cJun is commonly used as marker of JNK activity (57).

1.5. PPARγ and thiazolidinediones

Peroxisome proliferator-activated receptor γ (PPARγ) influences various metabolic pathways and is involved especially in fat cell biology (62). As a member of the nuclear receptor family, PPARγ is activated by direct binding of steroids, vitamins and lipid metabolites (63). In order to interact with the DNA, PPARγ binds the retinoic X receptor (RXR) and forms a heterodimer. In general the expression and activation of PPARγ is sufficient to stimulate adipogenesis (64). There are two PPARγ isoforms, called γ1 and γ2, with PPARγ2 being of higher molecular weight. While both isoforms can be found in adipocytes, only PPARγ1 is abundant in macrophages (63).

Thiazolidinediones, including rosiglitazone and pioglitazone, (TZDs) are anti-diabetic drugs, which function as strong synthetic PPARγ ligands. In general TZDs decrease the expression of adipokines as TNFα, IL-1 and resistin, which are associated with insulin resistance; the expression of adiponectin is increased by TZDs (65, 66). Nevertheless adverse long-term effects such as increased body weight, fluid retention and an increased risk of heart failure have been observed (67).

PPARγ stimulates the M2 polarization of adipose tissue macrophages (ATMs) and therefore influences insulin sensitivity (68). Moreover, activation of PPARγ by pioglitazone improves the unbalanced M1/M2 phenotype ratio of macrophages (69, 70) and leads to anti-diabetic effects. For further information, the reader is referred to the following publications: Lumeng, et al. (71), Bouhlel, et al. (69) and Fujisaka, et al. (70). Furthermore, PPARγ is a genetic sensor for free fatty acids (FFAs) (62, 63).

Using western blotting analysis FFAs, TNFα and IL-6 were identified as potent inducers of PPARγ phosphorylation. Moreover cyclin-dependent kinase 5 (Cdk5) was identified as inducer of PPARγ Ser273 phosphorylation (72), which results in the dysregulation of the expression profile of various genes. Furthermore, phosphorylation induced changes are comparable to gene expression profiles seen in obesity. A total of 17 genes was altered due to differential PPARγ phosphorylation.

1.6. Proteomics

Changes in the cellular conditions are reflected in alterations of gene expression which manifest on mRNA and protein level (73). Proteomics focus on proteins and especially on their structure and function. In the field of mass spectrometry the so-called 'shotgun' approach is quite common. While in a 'shotgun' approach, spectra from all detectable proteins are generated, the mass spectrometer is programmed to analyze only a preselected group of proteins in targeted proteomics. Quantitative proteomics requires the usage of stable labels, which can be brought in chemically or metabolically. Some of the commonly used techniques for labeling are isotope-coded affinity tags (ICAT), isobaric tags for relative and absolute quantitation (iTRAQ) and stable isotope labeling with amino acids in cell culture (SILAC). As the latter is going to be explained in detail, the reader is referred to the following publications for the former: Gygi, et al. (74) Ong and Mann (71), Mann (75) and Zieske (76).

1.6.1. Mass spectrometry

The workflow in mass spectrometry during a shotgun approach is depicted in Figure 6. In general, complex protein samples are digested to peptides which are further separated using reverse phase liquid chromotagraphy (RPLC) (Figure 6B). Before separation by column, peptides can be segregated using polyacrylamide gel electrophoresis and further processed by in-gel digestion. In order to trace posttranslational modifications such as phosphorylation, digested proteins can be enriched (Figure 6A). After separation by reverse phase chromatography, peptides are ionized by electrospray (ESI) directly in front of the mass spectrometer (Figure 6B). Afterwards the peptides are analyzed by mass spectrometry, which comprises two units (Figure 6C). At first a MS scan determines peptide intensity and mass to charge ratios (m/z). Moreover peptide

precursor ions are isolated and fragmented in MS/MS scans (77). Typically five to ten peptides are fragmented for each MS scan. Finally the peptides are identified using an amino acid sequence database. For detailed information on peptide sequencing the reader is referred to Steen and Mann (77).

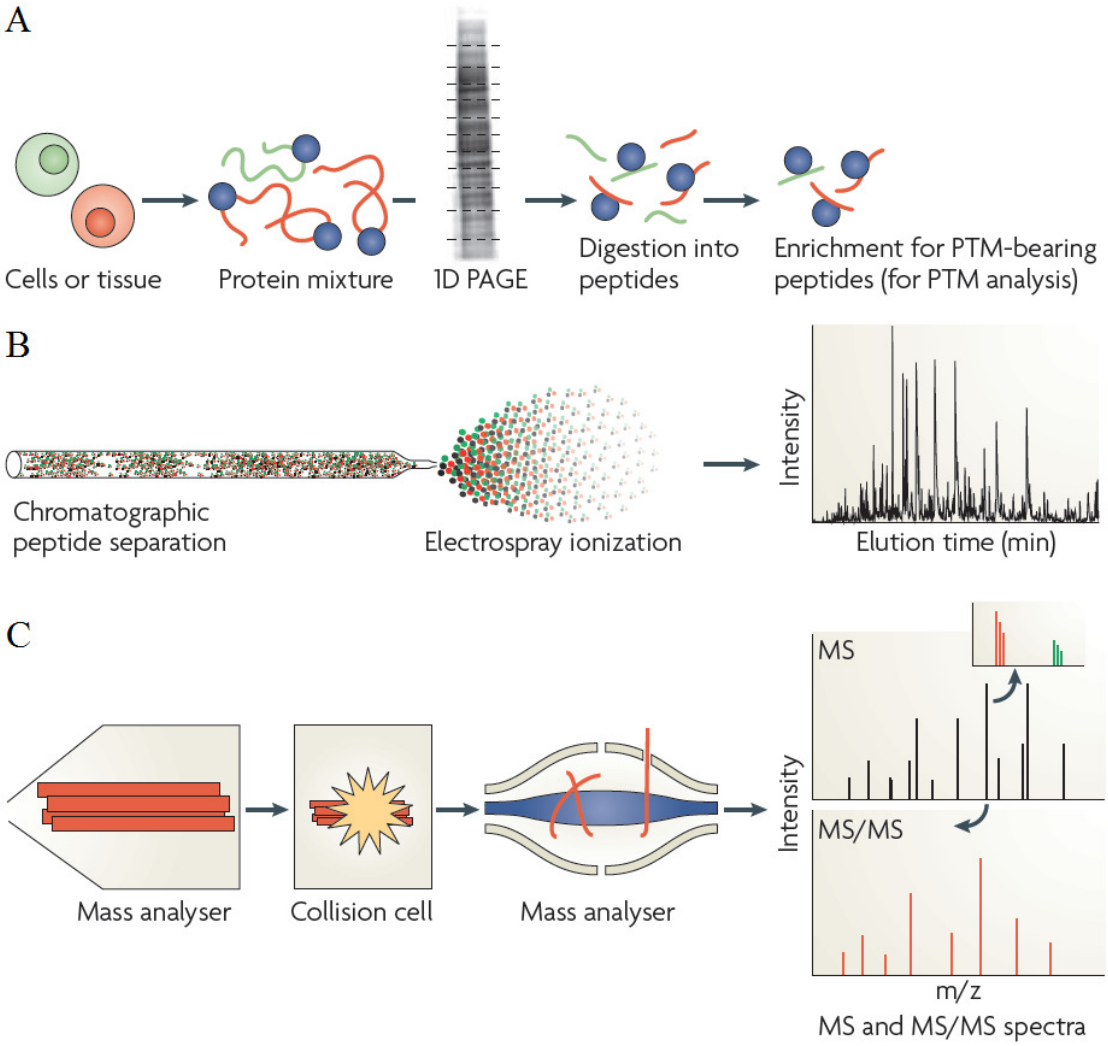

Figure 6: Workflow in mass spectrometry. (A) Extracted proteins are separated and 'in-gel digested' into peptides. Specific post-translational modifications can be enriched for quantification. (B) Purified peptides are separated by reverse phase chromatography and ionized by electrospray (ESI), directly in front of the mass spectrometer, after eluting from the column. (C) The ions are transferred to vacuum-containing mass spectrometer. The mass spectrometry (MS) mode is used to measure all ions at high resolution. Moreover, some peptide ions and fragments are selected for MS/MS scan. The results for stable isotope labeling by amino acids in cell culture (SILAC) are depicted in the inset in the MS panel. (adapted from Choudhary and Mann (78))

1.6.2. Stable-isotope labeling by amino acids in cell culture (SILAC)

Stable-isotope labeling by amino acids in cell culture (SILAC) was first described in 2002 (79) and is a method to metabolically label cells (Figure 7). In general two populations are grown, with one grown in 'normal' medium ('light') and the other grown in 'heavy' medium. The so-called 'heavy' medium is supplemented with heavy amino acids which were generated using ^{13}C or ^{13}N. In order to ensure the incorporation of the labeled amino acids, only essential amino acids (lysine or arginine) are chosen. Moreover, cells are grown in dialyzed medium and completely SILAC-labeled after five divisions. Fully labeled cells are mixed, their proteomes extracted and measured by MS. If lysine and arginine are used for labeling and trypsin is used for digestion, almost all peptides are labeled and can be used for further quantification. The incorporation of heavy amino acids into proteins results in a mass shift in the peptides. Therefore, peptides appear in pairs in mass spectra with the lower mass containing the light amino acid. A SILAC-ratio of one-to-one indicates, that there are no differences in the peptide abundance between both proteomes. Thus a higher heavy peak indicates more abundant peptides in the heavy labeled sample.

SILAC provides a way of metabolic labeling with stable isotopes without radioactivity where all samples can be processed together. Nevertheless SILAC was limited to whole proteome labeling via protein turnover. Furthermore, the point of mixture plays an important role for the quantitative accuracy since the latter is decreasing with the time after which samples are mixed. In order to overcome this limitation Geiger, et al. (80) suggested using a SILAC-labeled spike-in standard (see 1.6.2.1.SILAC as spike-in standard). Nowadays, SILAC has developed into a broadly used technique. Furthermore a combination of different SILAC-labeled cell lines, which is called super-SILAC mix, enables to simulate whole tissues (81). At the moment entirely SILAC-labeled tissues, organs and even mice are available (82). For further reading the following reference is recommended: Mann (75).

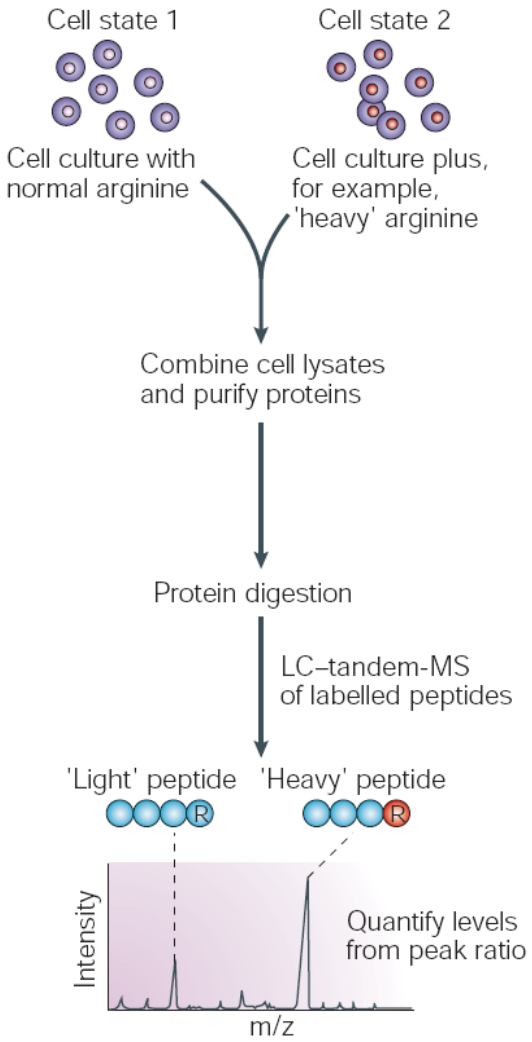

Figure 7: Relative quantification using stable-isotope labeling in cell culture (SILAC). One cell population is cultured in medium supplemented with a stably labeled amino acid ('heavy' arginine), which is incorporated into proteome. Furthermore a second population of cells is grown in normal media. After combination of both cell lysates, the sample is purified and the proteins digested. The peptide ratio is obtained for each mass spectrum and allows relative quantification. (77)

1.6.2.1. SILAC as spike-in standard

The general workflow of the recently published technique called spike-in SILAC (80) is depicted in Figure 8. The SILAC standard functions as 'heavy' SILAC component, whereas the sample functions as 'light' component. The standard is spiked into each of the samples, which are further processed together. As depicted in Figure 8 the standard can be produced separately and completely independent of the experiment. Therefore all experimental samples can be prepared without any restrictions in normal media and amino acids. Moreover the number of samples is no longer restricted to three as in classical SILAC, as the standard can be aliquotted and used multiple times. As the

standard is present in all samples, the peptide fold-change ratio between the samples is the ‘ratio of ratios’ (Figure 8). The mass shift has to be at least 4Da to prevent partially overlapping SILAC-pair.

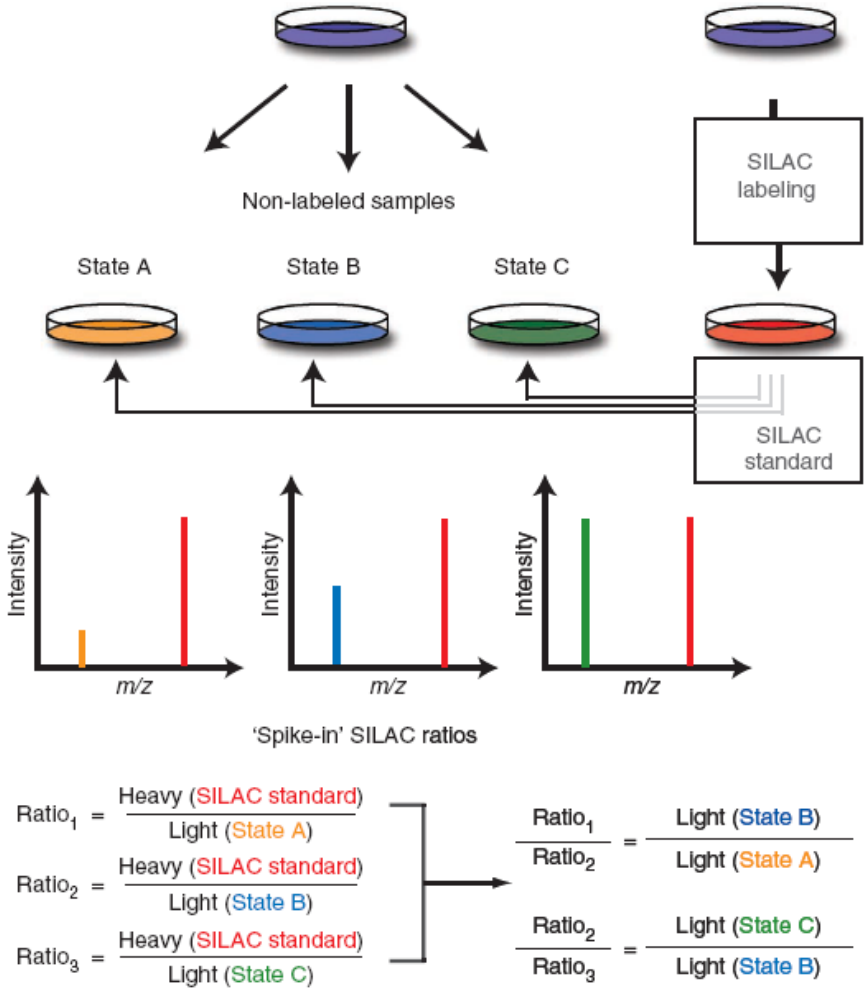

Figure 8: Workflow during spike-in SILAC. The spike-in SILAC standard enables a separation of labeling process and biological experiment. After the experiment the SILAC standard is mixed with each sample, each mix is analyzed separately. The difference between two experimental samples is obtained by dividing the ratio of one sample to the ratio of the other sample (both ratios relative to the standard). (80)

1.6.3. MaxQuant analysis

The MaxQuant software (version 1.0.13.13) is used to analyze large high-resolution mass spectrometric data sets. The LTQ Orbitrap software generated raw files, which are loaded into the so-called ‘Quant’ module. This module assembles the isotope patterns into SILAC pairs and generates two kinds of output files. Already processed MS/MS spectra are bundled together in ‘msm’ files whereas search engine parameters are

contained in ‘par’ files. Mascot is used as search engine. Finally the ‘identify’ module combines the search engine results with the raw file in order to assemble the peptides into proteins, quantify the proteins and write several tables containing the results. For a more detailed description the reader is referred to Cox and Mann (83) or Cox, et al. (84).

1.7. Aims of this master thesis

The aim of this master thesis is to use an in vitro coculture system composed of 3T3-L1 adipocytes and RAW264.7 macrophages in order to study the communication between these cell types. A schematic diagram of the utilized transwell coculture system is depicted in Figure 9. In general, 3T3-L1 adipocytes were seeded onto the bottom of the well while RAW264.7 macrophages were seeded into the transwell insert.

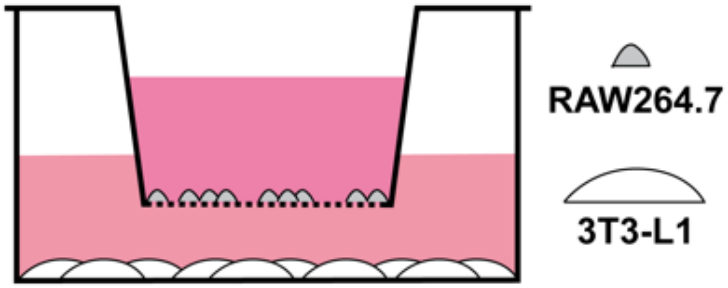

Figure 9: Schematic diagram of the coculture system.

A particular emphasis lies on enabling a proteome-wide detection of cell-cell communication by mass spectrometry. This includes the development of a suitable cell culture system and mass spectrometry detection. Furthermore, the adipocyte-macrophage communication shall be studied on the RNA-protein expression and metabolic level using specific marker molecules.

A workflow overview for the coculture experiments is depicted in Table 1. At first, a 6-well plate shall be used to determine optimal culture conditions using biomarkers such as free fatty acids and tumor necrosis factor α. Moreover, mRNA shall be extracted in order to study coculture-induced changes on RNA level. The knowledge from the 6-well experiments shall be used to establish a coculture system using 50cm² dishes.

These can be facilitated to investigate coculture-induced changes on protein level by mass spectrometry and western blotting.

system	culture	extraction of
6-well	control coculture coculture + palmitate	mRNA
50cm² dish	control coculture	protein

Table 1: Workflow for the coculture experiments.

2. Material and methods

2.1. Material

2.1.1. Chemicals and Enzymes

chemical/enzyme	company
3-Isobutyl-1-methylxanthine (IBMX)	Sigma-Aldrich (Taufkirchen, Germany)
Acetic acid	Merck (Darmstadt, Germany)
Acetonitrile	Roth (Karlsruhe, Germany)
Ammonium acetate	Merck (Darmstadt, Germany)
Ammoniumcarbonate	Sigma-Aldrich (Taufkirchen, Germany)
BSA	Sigma-Aldrich (Taufkirchen, Germany)
c-Jun (L70B11) Mouse mAb	Cell Signalling Technology (Danvers, USA)
Coomassie Brillant Blue R250	Bio-Rad Laboratories (München, Germany)
Dexamethasone	Sigma-Aldrich (Taufkirchen, Germany)
Dithiothreitol (DTT)	Sigma-Aldrich (Taufkirchen, Germany)
dNTP	Promega (Mannheim, Germany)
EGTA	Sigma-Aldrich (Taufkirchen, Germany)
Ethanol	Merck (Darmstadt, Germany)
Ethylenediaminetetraacetic acid (EDTA)	Sigma-Aldrich (Taufkirchen, Germany)
Formic acid	Merck (Darmstadt, Germany)
Glycerol	Sigma-Aldrich (Taufkirchen, Germany)
Glycin	Sigma-Aldrich (Taufkirchen, Germany)
Goat anti-mouse IgG-HRP: sc-2005	Santa Cruz (Heidelberg, Germany)
Goat anti-rabbit IgG-HRP: sc-2004	Santa Cruz (Heidelberg, Germany)
Insulin solution	Sigma-Aldrich (Taufkirchen, Germany)
Iodoacetamide	Serva (Heidelberg, Germany)
Isopropanol	Merck (Darmstadt, Germany)
JNK1 (2C6) Mouse mAb	Cell Signalling Technology (Danvers, USA)
Leupeptin	Serva (Heidelberg, Germany)
MagicMark (TM) XP Western	Invitrogen (Karlsruhe, Germany)

chemical/enzyme	company
Milk powder	Roth (Karlsruhe, Germany)
NuPAGE® MES SDS RunningBuffer (20X)	Invitrogen (Karlsruhe, Germany)
P-c-JUN (Ser63/73): sc-16312	Santa Cruz (Heidelberg, Germany)
Pepstatin A	Serva (Heidelberg, Germany)
Phosphatase Inhibitor Cocktail 2 (5 mL, 100x)	Sigma-Aldrich (Taufkirchen, Germany)
P-JNK (G-7): sc-6254	Santa Cruz (Heidelberg, Germany)
Polyoxyethylenesorbitanmonolaurate (Tween)	Sigma-Aldrich (Taufkirchen, Germany)
PPARγ (E-8): sc-7273	Santa Cruz (Heidelberg, Germany)
Precision Plus Protein all blue standards	Bio-Rad Laboratories (München, Germany)
Protease Inhibitor Cocktail Tablets	Roche (Mannheim, Germany)
Restore™ Plus Western Blot Stripping Buffer	Thermo Scientific (Bonn, Germany)
Sodium dodecyl sulfate (SDS)	Sigma-Aldrich (Taufkirchen, Germany)
Trichloroacetic acid (TCA)	Roth (Karlsruhe, Germany)
Trishydroxymethylaminomethane (Tris)	Sigma-Aldrich (Taufkirchen, Germany)
TrypLE™ Express	Gibco (Invitrogen, Karlsruhe, Germany)
Trypsin Sequencing Grade	Roche (Mannheim, Germany)
Western Lightning Plus ECL	Perkin Elmer (Rodgau, Germany)
β-Mercaptoethanol	Sigma-Aldrich (Taufkirchen, Germany)

2.1.2. Instruments

instrument/software	**company**
ABI Prism 7900HT System	Applied Biosystems (Darmstadt, Germany)
Bright-Line Counting Chamber	Hausser Scientific (Horsham, USA)
LTQ XL Orbitrap	Thermo Scientific (Bonn, Germany)
Nanodrop ND-1000	Nanodrop (Peqlab, Erlangen, Germany)
Nanoflow reverse phase liquid chromotagraphy (RPLC)	Agilent Technologies (Santa Clara, USA)

instrument/software	company
PCR cycler (PTC-200)	MJ Research, GMI Inc. (Ramsey, USA)
PicoFrit analytical column	New Obejectives (Woburn, USA)
POLARstar Omega	BMG LABTECH (Offenburg, Germany)
SDS 2.1	Applied Biosystems (Darmstadt, Germany)
Speed Vac Concentrator	Savant, Thermo Scientific (Bonn, Germany)

2.1.3. Consumables

consumable	**company**
24mm Transwell with 0.4µm Pore Polycarbonate Membrane Insert	Corning (Schwerte, Germany)
384-well plate (white, clear)	Greiner Bio-One (Frickenhausen, Germany)
384-well Plate, PS, Small Volume™, HiBase	Greiner Bio-One (Frickenhausen, Germany)
75mm Transwell with 0.4µm Pore Polycarbonate Membrane Insert	Corning (Schwerte, Germany)
96-well MultiScreen Ultracel filter plate	Millipore (Schwalbach, Germany)
Biozym LE Agarose	Biozym (Hessisch Oldendorf, Germany)
C 18 resin (Reprosil-AQ Pur)	Dr. Maisch (Ammerbuch-Entringen, Germany)
cell culture flask T150	Corning (Schwerte, Germany)
cell culture flask T25	Corning (Schwerte, Germany)
Costar® 6-well Clear TC-Treated Multiple Well Plates	Corning (Schwerte, Germany)
Dulbecco's Modified Eagle's Medium (DMEM)	ATCC (Wesel, Germany)
FBS Superior	Biochrom (Berlin, Germany)
low protein binding tube	Eppendorf (Hamburg, Deutschland)
MicroAmp Optical 384-Well Reaction Plate	Applied Biosystems (Darmstadt, Germany)

consumable	company
Nitrocellulose membrane	GE Healthcare (München, Germany)
NuPAGE Novex® 4-12% Bis-TrisGels	Invitrogen (Karlsruhe, Germany)
Pierce C18 Tips 100 µL (8-80 µg capacity)	Thermo Scientific (Bonn, Germany)

2.1.4. Molecular biological Kits

kit	**company**
CellTiter-Glo Luminescent Cell Viability Assay	Promega (Madison, USA)
Fatty acid quantification Kit	BioVision (Mountain View, USA)
High Capacitiy Rev.Transcription Kit, 1000 reactions	Applied Biosystems (Darmstadt, Germany)
Mouse TNF-α Ready-SET-Go! ELISA Kit	eBioscience (Frankfurt, Germany)
NE-PER Nuclear and Cytoplasmic Extraction Reagents	Thermo Scientific (Bonn, Germany)
Power SYBR® Green PCR Master Mix	Applied Biosystems (Darmstadt, Germany)
RNeasy® 96	Qiagen (Hilden, Germany)
Triglyceride quantification Kit	BioVision (Mountain View, USA)

2.2. Methods

2.2.1. Cultivation of 3T3-L1 adipocytes

The L1 substrain of the Swiss 3T3 mouse cell line (85) was utilized as adipocyte model system. Cells were kindly provided from Prof. Dr. Dr. H.-G. Joost (Deutsches Institut für Ernährunfsforschung (DIfE), Potsdam).

The 3T3-L1 cell line has a fibroblastic morphology and is one of the best characterized models of adipogenesis. Upon differentiation, confluent 3T3-L1 cells re-enter the cell cycle and adopt a rounded phenotype accompanied by the accumulation of lipid in droplets (86).

Preconfluent 3T3-L1 preadipocytes in a 150cm² flask were washed twice with 20ml PBS buffer after the medium was removed. Afterwards the cells were detached by adding 2ml TrypLE Express and incubated for 8 minutes at 37°C and 5% CO_2. Subsequently digestion was stopped by adding Dulbecco's Modified Eagle Medium (DMEM) supplemented with 10% fetal bovine serum (FBS) Superior. The cell suspension was centrifuged for 5 minutes at 180g. After discarding the supernatant the cell pellet was resuspended in 5ml DMEM/10% FBS. The 3T3-L1 cells were incubated at 37°C and 5% CO_2 until they reached confluence. Differentiation was initiated 1 day after 100% confluence was reached.

Confluent 3T3-L1 cells preadipocytes were treated with 50ml initiation medium containing 500µM IBMX, 10µM Dexamethasone, 10µg/ml insulin in DMEM/10% FBS. The 3T3-L1 cells were incubated with initiation medium for 2 days at 37°C and 5% CO_2. Afterwards, medium was changed to 40ml progression medium consisting of DMEM/10% FBS supplemented with 10µg/ml insulin. The 3T3-L1 cells were incubated with progression medium for 2 days at 37°C and 5% CO_2. Subsequently, medium was changed at day 6 and day 8 to 50ml fresh DMEM/10% FBS followed by another 2 day incubation at 37°C and 5% CO_2. Ten days after the initiation of differentiation, 3T3-L1 cells were ready for seeding or could be further cultivated in DMEM/10% FBS at 37°C and 5% CO_2.

2.2.2. Cultivation of RAW264.7 macrophages

As a macrophage model RAW264.7 mouse monocyte cells were purchased from Sigma-Aldrich Chemie GmbH. The utilized cell line was established from tumor ascites, which were induced in male mice by injection of Abselon Leukemia Virus (A-MulV). RAW264.7 cells are able to pinocytose neutral red and phagocytose zymosan. Furthermore, this cell line is capable of lysozyme production and growth inhibited by addition of 0.5ng/ml lipopolysaccharides (LPS, Figure 10). In addition RAW264.7 cells are tumorgenic when placed in mice (87).

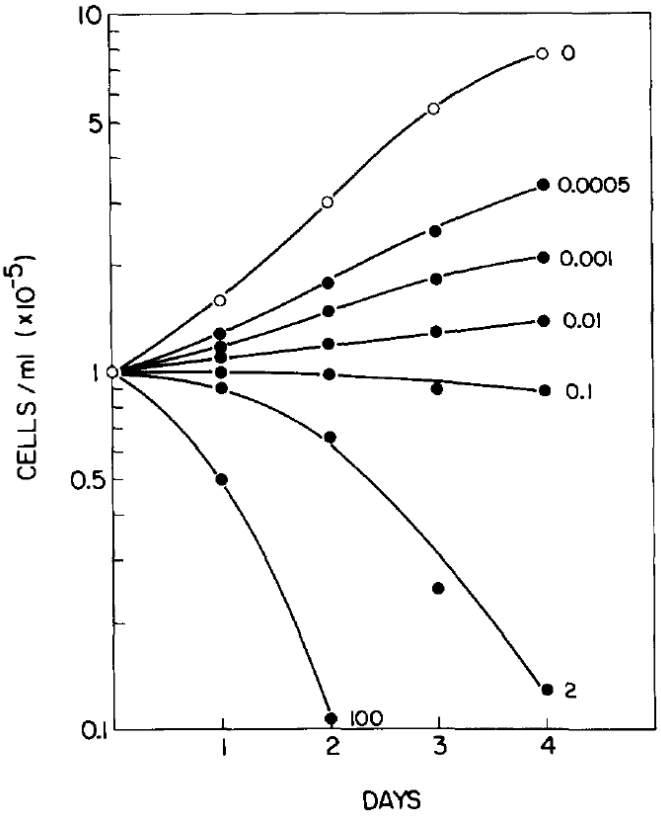

Figure 10: LPS induced growth inhibition of macrophage cell line RAW264.7. RAW264.7 were inhibited at 10^5 cells/ml, numbers indicate amount of LPS (µg(ml) added to the culture. Viability of the cells was determined on a daily basis. (87)

RAW264.7 macrophages were grown and cultured in DMEM/10% FBS at 37°C and 5% CO_2. In order to split the cells, they were scratched in 10ml DMEM/10% FBS and afterwards centrifuged for 5 minutes at 150g. After discarding the supernatant the pellet was resuspended in 10ml fresh medium (DMEM/10% FBS) and cells were seeded into a 150cm² flask. After 2 days RAW264.7 macrophages were scratched in

10ml DMEM/10% FBS and afterwards centrifuged for 5 minutes at 150g. After discarding the supernatant the pellet was resuspended in 10ml fresh medium ($2*10^6$ cells/ml).

2.2.3. Coculture of adipocytes and macrophages

For the coculture system, differentiated 3T3-L1 adipocytes were cocultured with RAW264.7 macrophages in DMEM/10% FBS for a maximum of 24 hours using 6-well plates containing transwell inserts with a 0.4m² porous membrane. Additionaly, 50cm² dishes containing transwell inserts were used as coculture system. RAW264.7 macrophages and 3T3-L1 adipocytes of equal numbers to those in the coculture were cultured separately as control cultures. The 6-well plate was used to determine optimal culture conditions in order to observe cocultural effects. Finally, these conditions were transferred to the 50cm² dishes. The conditions for the 6-well plates were the following: 3T3-L1 adipocytes were seeded with 50% confluence on the bottom of the well. Moreover, $1.1*10^4$ RAW264.7 macrophages/cm² were seeded into the insert and as control culture. After 4 hours, 8 hours and 24 hours of incubation, supernatants were collected, centrifuged for 10 minutes at 10,000g and 4°C; samples were stored at −20°C for further analysis. Furthermore, mRNA was collected at equal time points. While 3T3-L1 adipocytes were washed twice, RAW264.7 macrophages were only washed once with PBS. Afterwards 350µl RLT buffer were added to lyse the cells and the total volume was pipetted into a Eppendorf tube containing 3.5µl mercaptoethanol. The solution was vortexed and stored on ice until centrifugation for 10 minutes at 10,000g at 4°C. The sample was stored at -80°C until mRNA extraction.

The conditions for the 50cm² dishes were the following: 3T3-L1 adipocytes were seeded with 50% confluence; varying amounts of RAW264.7 macrophages ($1.7*10^4$ to $4.5*10^4$ macrophages per insert and cm²) were seeded into the insert while $7.5*10^5$ RAW264.7 macrophages per ml were seeded as control culture. After 8 hours and 24 hours of incubation, supernatants were collected, centrifuged for 10 minutes at 10,000g and 4°C; samples were stored at −20°C for further analysis. The results of the supernatant analysis were normalized to $1*10^6$ RAW264.7 macrophages seeded. Furthermore, proteins were collected at equal time points. Therefore, the remaining

medium was discarded and RAW264.7 macrophages were scratched off the membrane before centrifugation at 500g and 4°C for 5 minutes. Afterwards, the pellet was resuspended in ice cold PBS supplemented with protease inhibitor (1x) and phosphatase inhibitor (1x). Subsequently, the pellet was centrifuged for 5 minutes at 500g and 4°C. Finally, the pellet was resolved in ice cold PBS supplemented with protease inhibitor (1x) and phosphatase inhibitor (1x) and transferred into an low protein binding Eppendorf tube. At last, the tube was centrifuged at 10,000g for 5 minutes at 4°C; after discarding the supernatant the pellet was stored at -80°C. 3T3-L1 adipocytes were washed twice with PBS before being scratched off in ice cold PBS supplemented with protease inhibitor (1x) and phosphatase inhibitor (1x). Subsequently the pellet was centrifuged for 5 minutes at 500g and 4°C before the supernatant was discarded once more. Finally the pellet was resolved in ice cold PBS supplemented with protease inhibitor (1x) and phosphatase inhibitor (1x) and transferred into a low protein binding Eppendorf tube. At last the tube was centrifuged at 10,000g for 5 minutes at 4°C; after discarding the supernatant the pellet was stored at -80°C.

2.2.4. CellTiterGlo® Luminescent Cell Viability Assay

In order to monitor the viability of RAW264.7 macrophrages in presence of free fatty acids (FFAs) the CellTiter-Glo® Luminescent Cell Viability Assay was used. The number of viable cells in culture was assessed via the quantification of adenosine-5'-triphosphate (ATP), which is characteristic for metabolically active cells. The generated luminescence signal is proportional to the amount of ATP present (88).

At first 25µl DMEM/10% FBS containing $2.5*10^3$ RAW264.7 macrophages were pipetted per well of a 384-well plate. The next day additional 25µl DMEM/10% FBS containing a certain FFA concentration were added to each well and followed by a 24 hour incubation. The visual condition of the macrophages was documented, before the plate was equilibrated for 30 minutes at room temperature. After addition of 20µl CellTiter-Glo® reagent to each well, the plate was centrifuged for 1 minute at 10g. Moreover, the 384-well plate was shaken for 2 minutes using the POLARstar Omega and afterwards centrifuged for 1 minute at 10g before luminescence measurement with the POLARstar Omega. Data are presented in mean ± S.D., furthermore statistical analysis was performed by using a two-tailed Student’s t test.

2.2.5. Tumor necrosis factor α (TNFα) quantification

Tumor necrosis factor α (TNFα) is a multifunctional cytokine with the ability to interfere especially with the adipocyte metabolism. TNFα influences various sites including transcriptional regulation, glucose and fatty acid metabolism (40).

In order to assess the amount of TNFα the Mouse TNF-α Ready-SET-Go! ELISA Kit from eBioscience was utilized. The assay allows measuring TNFα levels in the supernatant via performing a quantitative enzyme linked immunosorbent assays (ELISA). In detail, a Corning Costar ELISA plate was coated using a mixture of capture antibody and coating buffer. Afterwards the plate was sealed and incubated at 4°C over night. The following day all wells were aspirated and washed 5 times with wash buffer; to increase the effectiveness of the washes all wells were incubated 1 minute before starting another wash. The plate was blotted on absorbent paper to remove residual buffer. After blocking the wells using blocking buffer, the plate was sealed once more and incubated for 1 hour at room temperature. Afterwards all wells were aspirated and washed 5 times with wash buffer; to increase the effectiveness of the washes all wells were incubated 1 minute before starting another wash. The plate was blotted on absorbent paper to remove residual buffer. After adding the samples the plate was incubated 3.5 hours at room temperature. Next the plate was aspirated and washed five times as previously described. Afterwards detection buffer was added and the plate was incubated for 1 hour at room temperature before aspirating and further washes (five times as previously described). Subsequently enzyme buffer was added and the sealed plate was incubated at room temperature for 30 minutes before all wells were aspirated and washed (7 washes, 2 minutes incubation time for each wash). After adding the substrate solution the plate was incubated for 30 minutes prior to stopping the reaction by adding stop solution. Finally the absorbance was measured at 470nm using the POLARstar Omega. In order to reduce the background, absorbance values at 570nm were subtracted from those at 450nm prior to data analysis. All samples were run as triplicate. Data are presented in mean ± S.D.

2.2.6. Free fatty acid quantification

Free fatty acids (FFAs) play a very important role in normal metabolism and in the development of many diseases. They are precursors of numerous bioactive compounds and have been reported to play a role in inflammation response.

In order to assess the amount of free fatty acids the Free Fatty Acids Quantitation Kit was utilized according to the manufacturer's protocol. The enzyme-based assay enables the detection of long-chain FFAs. After converting the fatty acids into their CoA derivative, the oxidization of the derivative generates a colorimetric signal. In detail the protocol included the following steps: ACS reagent was diluted with assay buffer and aliquotted according to the number of samples. Afterwards the samples as well as the standards were added to the mix. The solutions were vortexed and centrifuged for 30 seconds at 1,000rpm at room temperature. Subsequently samples were incubated for 30 minutes at 37°C using the PCR cycler. During incubation time a second mix consisting of assay buffer, fatty acid probe, enzyme mix and enhancer was prepared, which was then added to each sample. The samples were centrifuged for 30 seconds at 1,000rpm at room temperature before incubating for 30 minutes at 37°C using the PCR cycler. Finally the samples were transferred into a Greiner bio-one 384-well plate (Small Volume™, HiBase). After 30 seconds of centrifugation at 1,000rpm the absorbance was measured at 570nm using the POLARstar Omega. In order to reduce the background, absorbance values at 670nm were subtracted from those at 570nm prior to data analysis. All samples were run as triplicate. Data are presented in mean ± S.D.

2.2.7. Triglyceride quantification

Triglycerides (TG) serve as energy source and can be broken down into fatty acids and glycerol; both are known substrates for energy producing and metabolic pathways. In order to assess the amount of triglycerides the Triglyceride Quantitation Kit from BioVision was utilized according to the manufacturer's protocol. The enzyme-based assay enables the detection of triglycerides. After converting the triglycerides into free fatty acids and glycerol, the oxidization of the glycerol generates a colorimetric signal.

In detail the protocol includes the following steps: Lipase was diluted with assay buffer and aliquotted according to the number of samples. Afterwards the samples as well as

the standards for the standard curve were added to the mix. The solutions were vortexed and centrifuged for 30 seconds at 1,000rpm at room temperature. Subsequently the samples were incubated for 20 minutes at room temperature. During incubation time a second mix consisting of assay buffer, triglyceride probe and enzyme mix was prepared, which was then added to each sample. The samples were centrifuged for 30 seconds at 1,000rpm before incubating for 60 minutes at room temperature. Finally the samples were transferred into a Greiner bio-one 384-well plate (Small Volume™, HiBase). After 30 seconds of centrifugation at 1,000rpm the absorbance was measured at 570nm using the POLARstar Omega. In order to reduce the background, absorbance values at 670nm were subtracted from those at 570nm prior to data analysis. All samples were run as triplicate. Data are presented in mean ± S.D.

2.2.8. Real-time polymerase chain reaction

Gene expression analysis provides specific information concerning molecular effects of the crosstalk between 3T3-L1 adipocytes and RAW264.7 macrophages. This is due to the fact, that stimulating or inhibiting signals result in changes of gene transcription (40). Therefore putative changes in gene expression were examined for important genes using real-time polymerase chain reaction (qPCR). The total mouse RNA from 3T3-L1 adipocytes and RAW264.7 macrophages was isolated using the RNeasy® 96 Kit according to the manual. RNA was eluted in 45µl RNase-free water. To determine the amount of isolated RNA the light absorbance at 260nm was determined using a Nanodrop 1000. RNA quality was assessed by the absorbance ratios of 260nm/280nm and 260nm/230nm. Isolated RNA was stored at -70°C. Furthermore, cDNA of the extracted mRNA, was produced by reverse transcription using the High Capacity cDNA Reverse Transcription Kit according to the manufacturer's instructions. In detail, reverse transcription was carried out with 1µg RNA template, 10x RT buffer, 10x RT random primers, 25x dNTP mix (100mM), MultiScribe™ Reverse Transcriptase and RNase Inhibitor. The following program was performed: 10 minutes at 25°C, 120 minutes at 37°C, 5 seconds at 85°C and afterwards cool down to 4°C. cDNA was stored at -20°C.

Real-time PCR was performed with Power SYBR® Green PCR Master Mix, according to the manufacturer's protocol on an ABI Prism 7900 HT Fast Real-Time PCR System. In order to prevent variations within the assay, the sample cDNA was premixed with Power SYBR® Green PCR Master Mix and afterwards distributed equally to each well. Moreover, 0.5µM of each primer pair was used. Real-time PCR was performed in 5µl with the following cycling parameters: 95°C for 10 minutes, 40 cycles of PCR (95°C for 15 seconds, 60°C for 1 minute), 95°C for 15 seconds, 60°C for 15 seconds and 95°C for 15 seconds. As a reference gene, the mRNA level of β-actin was determined in real-time PCR for each RNA sample and further used to normalise gene expression levels. Quantification was done using the $2^{-\Delta\Delta Ct}$ method (89). All samples were run as technical triplicate. Relative gene expression values describe up- (>1) or downregulation (<1) of RNA expression. Data are presented in mean ± S.D., furthermore statistical analysis was performed by using a two-tailed Student's t test. The PCR primers used are listed in Table 2.

gene	sense strand	antisense strand
Acyl	5'-CAGCCAAGGCAATTTCAGAGC-3'	5'-CTCGACGTTTGATTAACTGGTCT-3'
Adipo (Adiponectin)	5'-AGGAAAGGAGAGCCTGGAGA-3'	5'-CGAATGGGTACATTGGGAAC-3'
Adipsin	5'-CATGCTCGGCCCTACATGG-3'	5'-CACAGAGTCGTCATCCGTCAC-3'
Aplp2	5'-GTGGTGGAAGACCGTGACTAC-3'	5'-TCGGGGGAACTTTAACATCGT-3'
Car3	5'-TGACAGGTCTATGCTGAGGGG-3'	5'-CAGCGTATTTTACTCCGTCCAC-3'
Cd24a	5'-GTTGCACCGTTTCCCGGTAA-3'	5'-CCCCTCTGGTGGTAGCGTTA-3'
Cidec	5'-ATGGACTACGCCATGAAGTCT-3'	5'-CGGTGCTAACACGACAGGG-3'
Cox-2	5'-CCCTGCTGCCCGACACCTTC-3'	5'-CCAGCAACCCGGCCAGCAAT-3'
Cyp2f2	5'-GTCGGTGTTCACGGTGTACC-3'	5'-AAAGTTCCGCAGGATTTGGAC-3'
Ddx17	5'-TCTTCAGCCAACAATCCCAATC-3'	5'-GGCTCTATCGGTTTCACTACG-3'
Fabp4	5'-TGATGCCTTTGTGGGAACCT-3'	5'-GCAAAGCCCACTCCCACTT-3'
Glut4	5'-GCGGATGCTATGGGTCCTTA-3'	5'-GTCCGGCCTCTGGTTTCA-3'
Il-1b	5'-GGACCCCAAAAGATGAAGGGCTGC-3'	5'-GCCACAGCTTCTCCACAGCCA-3'
Il-6	5'-TCTGCAAGAGACTTCCATCCAGTTGC-3'	5'-AGGCCGTGGTTGTCACCAGC-3'
Mcp-1	5'-CCAGCACCAGCACCAGCCAA-3'	5'-TGGGGCGTTAACTGCATCTGGC-3'
Mincle	5'-ACCAAATCGCCTGCATCC-3'	5'-CACTTGGGAGTTTTTGAAGCATC-3'
Nr1d1	5'-TACATTGGCTCTAGTGGCTCC-3'	5'-CAGTAGGTGATGGTGGGAAGTA-3'
Nr1d2	5'-TGAACGCAGGAGGTGTGATTG-3'	5'-GAGGACTGGAAGCTATTCTCAGA-3'
Nr3c1	5'-AGCTCCCCCTGGTAGAGAC-3'	5'-GGTGAAGACGCAGAAACCTTG-3'
Peg10	5'-TGCTTGCACAGAGCTACAGTC-3'	5'-AGTTTGGGATAGGGGCTGCT-3'
Rarres2	5'-GCCTGGCCTGCATTAAAATGG-3'	5'-CTTGCTTCAGAATTGGGCAGT-3'
Resistin	5'-CCTCTGCCACGTACCCACGG-3'	5'-ACAGTGGCATGCTGGAGCCC-3'
Rybp	5'-CGACCAGGCCAAAAAGACAAG-3'	5'-CACATCGCAGATGCTGCATT-3'
Selenbp1	5'-ATGGCTACAAAATGCACAAAGTG-3'	5'-CCTGTGTTCCGGTAAATGCAG-3'
Tnfα	5'-AGCCCACGTCGTAGCAAACCA-3'	5'-CATGCCGTTGGCCAGGAGGG-3'
Txnip	5'-TCTTTTGAGGTGGTCTTCAACG-3'	5'-GCTTTGACTCGGGTAACTTCACA-3'
β-actin	5'-CGTGAAAAGATGACCCAGAT-3'	5'-CCATCACAATGCCTGTGGTA-3'

Table 2: Primers utilized for real-time polymerase chain reaction (PCR).

2.2.9. Western blotting

Each sample was mixed with 4x NuPAGE® LDS sample buffer and dithiothreitol (DTT) according to the manufacturer's protocol. Afterwards samples were incubated in the PCR cycler for 10 minutes at 70°C. Furthermore running buffer using 20x NuPAGE® MES SDS Running Buffer was prepared following manufacturer's protocol. As marker equal volumes of MagicMark^{TM} XP Western Protein Standard and Precision Plus Protein Dual Color Standard were mixed. Moreover, 5µl marker and 10µl per sample were loaded on a NuPAGE gradient gel (4%-12% Bis-Tris gel). The gel was run at ~100V while the blotting buffer containing glycin and trishydroxymethylaminomethane (tris) was prepared. A nitrocellulose membrane from

GE Healthcare with 0.45µm pore size was utilized for blotting and treated according to the manufacturer's protocol. After 2 hours of blotting at 400mA in the cold room, the membrane was stained with PonceauS and the gel was stained with Coomassie brilliant blue. Afterwards the membrane was destained by several washes with water. For each antibody a specific blocking solution was utilized (Table 3) to which phosphatase stop (1x) was added. The membrane was incubated for 1 hour at room temperature. The first antibody (Table 4) was incubated over night at 4°C in blocking solution. Before applying the secondary antibody, the membrane was washed with TBS (50mM Trishydroxymethylaminomethane, 150mM sodium chloride, pH 7.6) supplemented with Polyoxyethylenesorbitanmonolaurate (Tween). The washing procedure lasted 10 minutes and was repeated two times.

	JNK	**cJun**	**IRS-1**	**β-actin**
Blocking solution	5% milk powder in 1x TBS + 0.05% Tween	5% milk powder in 1x TBS + 0.1% Tween	5% milk powder in 1x TBS + 0.1% Tween	1.5% milk + 1.5% BSA in 1xTBS + 0.1% Tween
Washing solution	1x TBS + 0.05% Tween	1x TBS + 0.1% Tween	1x TBS + 0.1% Tween	1xTBS + 0.1% Tween

Table 3: Blocking and washing solution utilized for western blotting.

The secondary antibody was incubated for 1 hour at room temperature in blocking solution. Before the detection, the membrane was washed with TBS+Tween for 10 minutes which was repeated two times. Western Lightning Chemiluminescence Plus and the Fuji-LAS-1000 were used for detection. Afterwards the membrane was washed for 15 minutes with TBS+Tween. In order to strip the membrane and enable application of the next antibody, the membrane was incubated for 10 minutes at room temperature in Restore™ Plus Western Blot Stripping Buffer. The membrane was washed with TBS+Tween for 10 minutes, which was repeated two times, before stripping effectiveness was tested via detection for 30 minutes. Finally, the membrane was blocked once more and the next antibody could be applied. The intensity of the detected bands was analyzed using the Freeware Software GelAnalyzer 2010.

	antibody	supplier	trade name
1st	JNK	Cell signaling	mouse JNK1 (2C6)
	P-JNK	Santa Cruz	mouse p-JNK (G-7)
	cJun	Cell signaling	mouse c-Jun (L70B11)
	P-cJun	Santa Cruz	rabbit p-c-JUN (Ser63/73)
	IRS-1	Cell signaling	rabbit IRS-1
	P-IRS-1	Santa Cruz	rabbit p-IRS-1 (Ser307)
	β-Actin	Santa Cruz	mouse b-Actin (C4)
2nd		Santa Cruz	goat anti-rabbit IgG-HRP
		Santa Cruz	goat anti-mouse IgG-HRP

Table 4: Antibodies utilized for western blotting.

2.2.10. Mass spectrometry analysis

The protein pellet deprived from 50cm² cultures was resuspended in a appropiate volume of complete UEES lysis (9 M Urea, 100 mM EDTA/EGTA, 4% SDS) buffer (pH 7.5), furthermore protease inhibitor (1x) and phosphatase (1x) stop were added before sonification. The lysates were sonificated using the MS 73 sonification tip and a Brandelin plus sonificator. The settings were the following 40% power, cycle 5 and 5 seconds. The sonification process was performed twice; samples were placed on ice in between. Finally all samples were stored at -20°C until further treatment.

2.2.10.1. In-gel digestion

At first 7µl of each sample was run on a 10% SDS Page and three evenly sized gel pieces per lane were cut out at random. Each slice was cropped into small pieces not larger than 1mm³ and placed into a low protein binding Eppendorf tube. The in-gel trypsin digestion was conducted according to the protocol of Kaiser, et al. (90). In brief, 25mM NH_4HCO_3 in 50% (v/v) acetonitrile (ACN) was added, in order to cover the gel pieces, which were further vortexed for 10 minutes. Subsequently the gel pieces were pelleted via centrifugation at 16,000g for 1 minute. After discarding the supernatant the

procedure was repeated twice, before the pieces were completely dried using the Speed Vac Concentrator. Subsequently 10mM DTT in 25mM NH_4HCO_3 was added, vortexed and centrifuged at 16,000g, before allowing the reduction reaction to process at 56°C for 1 hour. Afterwards the supernatant was removed and 55mM iodoacetamide was added to cover the gel pieces. Subsequently, the samples were vortexed and centrifuged at 16,000g previous to allowing the alkylation reaction to proceed in the dark at room temperature for 45 minutes. The samples were vortexed and centrifuged occasionally during the incubation. Afterwards the supernatant was discarded and the pieces were washed in NH_4HCO_3 while vortexing for 10 minutes. Subsequently, the samples were centrifuged at 16,000g for 30 seconds; the supernatant was discarded and 25mM NH_4HCO_3 in 50% (v/v) ACN was added to cover the gel pieces. After vortexing for 5 minutes the samples were centrifuged 16,000g for 30 seconds and the procedure of adding 25mM NH_4HCO_3 in 50% (v/v) ACN was repeated once more. Finally, the gel pieces were dried completely before 5µl–10µl trypsin (10ng/µl) and 10% (v/v) ACN were added to each sample. After the gel pieces rehydrated a few minutes, 25mM NH_4HCO_3 was added to cover them. Before the pH was adjusted to pH 8, the samples were vortexed for 5 minutes and centrifuged for 30 seconds at 16,000g. Subsequently the samples were incubated at 37°C over night. The next morning, the gel pieces were centrifuged at 16,000g for 30 seconds and water was added prior to vortexing for 10 minutes followed by 30 seconds of centrifugation at 16,000g. The supernatant (digest solution) was transferred into a new low protein binding Eppendorf tube while 50% (v/v) ACN/5% (v/v) formic acid were added to the gel pieces to cover them. Afterwards the gel samples were vortexed for 10 minutes, before centrifugation at 16,000g for 30 seconds. The supernatant was transferred into the low protein binding Eppendorf containing the digest solution. The procedure of 50% (v/v) ACN/5% (v/v) formic acid addition was repeated once more. Finally, 100% (v/v) ACN was added to cover the gel pieces previous to vortexing for 5 minutes and centrifugation at 16,000g for 30 seconds. The supernatant was transferred into the low protein binding Eppendorf tube containing the digest solution. Subsequently, the digest solution was centrifuged at 16,000g for 30 seconds and the volume was reduced to 5µl–10µl using the Speed Vac Concentrator. Finally, the samples were centrifuged at 16,000g for 10 minutes and the supernatant was transferred into a new low protein binding Eppendorf tube. Each

sample was dissolved in 0.1% (v/v) formic acid and (5µl of 20µl) were utilized for LC-MS analysis. Each sample was run twice without a wash in between.

2.2.10.2. SILAC quantification

For the quantitative analysis the recently published method of SILAC-labeled spike-in standard (80) was utilized. This method provides the opportunity to decouple the coculture experiments from the labeling process. Therefore fully SILAC-labeled RAW264.7 macrophages and 3T3-L1 adipocytes were used as internal SILAC standard. Both standards contained Lys4 and Arg6. Therefore a mass shift of 4Da, 6Da or 10Da and multiples was expected. The internal standards were processed in the same way as the samples.

In order to reduce the sample 50µl were taken and 50mM ammonium bicarbonate was added to a total volume of 80µl. Afterwards 1M DTT was added and the samples were boiled for 5 minutes with the help of the shaker. All samples were placed one ice for 2 minutes, further 500mM iodoacetamid was added and the alkylation was allowed to progress for 30 minutes in the dark at room temperature. Subsequently, the samples were precipitated using 50% trichloroacetic acid (f.c.20% in bidest., TCA) and stored on ice for 15 minutes. After a 10 minute centrifugation at 20,000g at room temperature the supernatant was discarded. In order to wash the pellet 10% TCA was added before another centrifugation at 20,000g for 5 minutes at room temperature. The supernatant was discarded once more and Millipore water was added to wash the pellet. After centrifugation at 20,000g for 5 minutes the supernatant was discarded and the whole washing procedure was repeated twice. The samples were digested using trypsin solution, the reaction took place over night for at least 18 hours at 37°C in the shaker. The pH was monitored at the beginning of the digestion and measured the next day in the morning. In order to stop trypsination 0.5% formic acid was added to all samples. Furthermore, all samples were processed using 100µl C18 Tips. At first the tip was wetted using 100% ACN, the solvent was discarded afterwards and the procedure was repeated twice. The tip was equilibrated with 0.1% formic acid, which was discarded afterwards; the procedure was repeated twice. Subsequently the sample pipetted up and down before the tip was washed with 0.1% formic acid/5% ACN. The procedure was repeated twice. Finally, the sample was eluted into 0.1% formic acid in

80% ACN. After drying, the sample via Speed Vac Concentrator, the peptides were resolved in 5% ACN/2% formic acid. It was important to dissolve the peptides for at least
10 minutes in order to prevent precipitation on the column. In the end, the low protein binding Eppendorf tube was centrifuged 10 minutes at 10,000g and 4°C before the supernatant was transferred into a new low protein binding Eppendorf tube. After mixing each sample with the corresponding internal SILAC standard they were ready for LTQ Orbitrap measurement.

2.2.10.3. LTQ Orbitrap measurement

MS analysis was performed using a nanoflow reverse phase liquid chromotagraphy (RPLC) system which was coupled online to a Linear Ion Trap (LTQ) Orbitrap XL mass spectrometer.

The peptides were separated using a PicoFrit analyital column (75µm ID x 150mm long, 15µm Tip ID), which was in-house packed with a 3µm C18 resin. Peptides were eluted using a non-linear gradient over 160min at a flow rate of 200nl/min (solvent A: 97.9% H_2O, 2% acetonitrile, 0.1% formic acid; solvent B: 97.7% acetonitrile, 2% H_2O, 0.1% formic acid). For nanoelectrospray generation 1.8kV was applied. One full FT scan mass spectrum (300-2,000 m/z, resolution of 60,000 at m/z 400) was followed by 10 data-dependent MS/MS acquired in the linear ion trap with normalized collision energy (setting of 35%). All target ions already selected for MS/MS were dynamically excluded for 60 seconds.

2.2.10.4. Data analysis

Raw files generated by the LTQ Orbitrap were analyzed with MaxQuant version 1.0.13.13 (83). MS/MS spectra were searched using the Mascot search engine (version 2.2.2, Matrix Science) against the decoy International Protein Index (IPI)-mouse database (version 3.48). In order to be 99% confident at the peptide level, the cutoff value was set to 1%. As SILAC modifications $^{2}H_4$-labeled lysine (Lys4) and $^{13}C_6$-labeled arginine (Arg6) were used. The search included the following variable modification: protein N-terminal acetylation and methionine oxidation; further

carbamidomethylation at cycteine was included as fixed modification. Trypsin was set with a maximum of 2 missed cleavage sites. Two peptides, one of them being unique, were sufficient for identification. For quantification 2 unique peptides were necessary. A quantitative up- or down-regulation of protein (H/L ratio) between the samples was calculated as following: $\frac{\frac{sample\ 1}{SILAC}}{\frac{sample\ 2}{SILAC}}$ (ratio of ratios).

3. Results

3.1. Cytotoxicity assay

In order to assess the influence of free fatty acids on the viability of RAW264.7 macrophages a cytotoxicity assay was conducted using a 384-well plate (clear, white). Therefore RAW264.7 macrophages were incubated for 24 hours with varying palmitate concentrations (Figure 11). Afterwards the viability of the cells was determined using the CellTiterGlo Luminescent Cell Viability Assay (Promega). Results are depicted in Figure 11A.

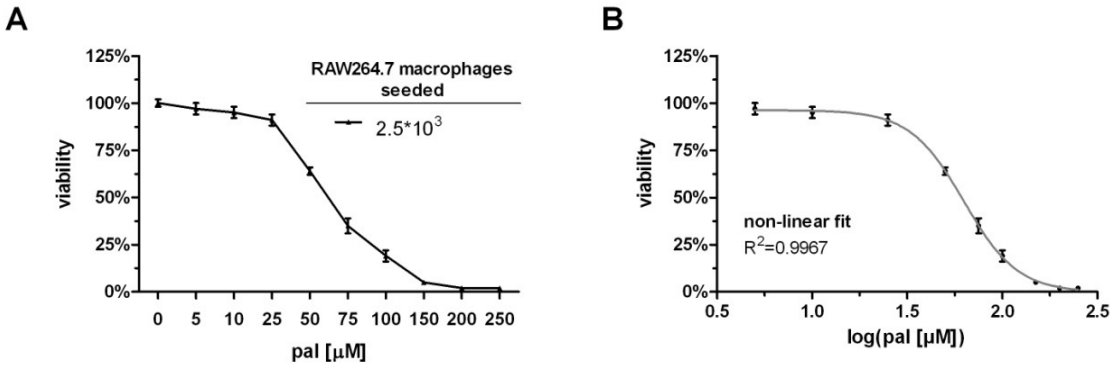

Figure 11: Dose-dependent decrease of viability of RAW264.7 macrophages after 24 hours treatment with palmitate. (A) Results of the cytotoxicity assay for $2.5*10^3$ RAW264.7 macrophages per well seeded. (B) Non-linear curve fit. pal, palmitate; error bars, S.D.; (n=4).

A decrease in cell viability was monitored depending on the palmitate concentration. Using a non-linear curve fit the palmitate concentration, where the viability is reduced to 90% was determined with 30.65 ± 1.04µM palmitate (Figure 11B). The goodness of the fit was verified using the coefficient of determination (R^2), which ranges from 0 to 1.

In accordance to the cytotoxicity assay, a maximum of 30µM palmitate was added in cell culture in order to stimulate the paracrine loop between adipocytes and macrophages (1).

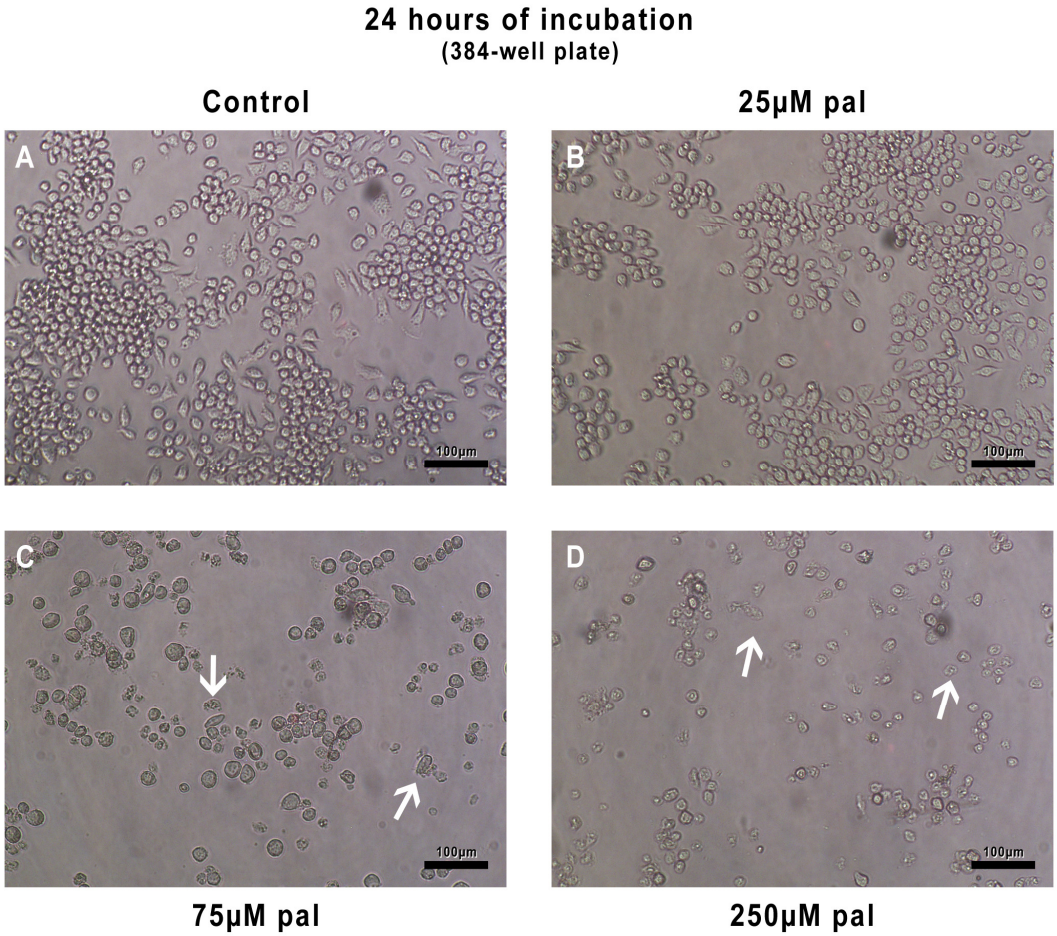

Figure 12: Dose-dependent decrease of RAW264.7 macrophages ($2.5*10^3$ cells per well seeded) viability after 24 hours of treatment with palmitate. (A) Control population of RAW264.7 macrophages. (B) Incubation of RAW264.7 macrophages in presence of 25µM palmitate resulted in a slightly decreased cell number. (C) Addition of 75µM palmitate resulted in markedly decreased cell number. Additionally, cell shape and integrity are disturbed (indicated by arrows). (D) Exposure of RAW264.7 macrophages to 250µM palmitate resulted in an enormous decrease in cell number as well as accumulation of disturbances in cell shape and integrity (indicated by arrows). pal, palmitate.

The results of the cytotoxicity assay correspond to microscopial observations (Figure 12). While there seems to be only a slightly decreased cell number after 24 hours of treatment with 25µM palmitate (Figure 12B), the cell number is considerably decreased in presence of 75µM palmitate (Figure 12C). Additionally, cell shape is changed due to less adhesion and the integrity of the unit is lost because of cell death (indicated by arrows in Figure 12C). In presence of 250µM palmitate (Figure 12D), the maximal concentration tested, cell number is decreased even further and the majority of the macrophages is no longer adherent (indicated by arrows in Figure 12D).

3.2. Cocultural effects

3.2.1. Experimental set-up in small dimension (6-well plate)

Using the 6-well plate coculture experiments can be conducted in small dimensions. Due to the conditions in the transwell system, 3T3-L1 adipocytes and RAW264.7 macrophages are seeded in the following ratio:

$$\frac{3T3\text{-}L1\ cells}{RAW264.7\ cells} = \frac{1.1*10^4 cells/cm^2}{3.0*10^4 cells/cm^2} = \frac{2.9*10^5\ cells}{5.1*10^4\ cells} = 5.7\ .$$

The conditions in the 6-well plate were studied by microscopy and by using biomarkers such as the free fatty acid and triglyceride concentration in the supernatant. Moreover, the tumor necrosis factor α level was assessed by a quantitative enzyme linked immunosorbent assays (ELISA). In addition, mRNA was extracted in order to study coculture-induced changes on RNA level.

Due to the influence of free fatty acids (FFAs) on the macrophage viability, it is important to monitor the RAW264.7 cells microscopically. Moreover, supposed lipolysis events can be examined in 3T3-L1 adiopocytes or in coculture. Microscopial observations of RAW264.7 macrophages, 3T3-L1 adipocytes and cocultured 3T3-L1 adipocytes are depicted in Figure 13. All pictures were taken after 24 hours of incubation.

3T3-L1 adipocytes can be identified by their characteristic appearance. The most striking feature is the large number of lipid droplets of different sizes, which are located within each cell (Figure 13A). The addition of 30µM palmitate causes only minor optical changes; in general the lipid droplets seem slightly bigger compared to the control (Figure 13B). The changes caused by the addition of 250µM palmitate are very obvious, as the lipid droplets increase markedly in size (Figure 13C). These findings suggest that 3T3-L1 adipocytes took up palmitate in order to store it in lipid droplets. RAW264.7 macrophages exhibit only minor optical changes in presence of 30µM palmitate (Figure 13E); the cell number seems to be slightly decreased. The addition of 250µM palmitate resulted in a noticeably decreased cell number. These results are in agreement with the cytotoxicity assay.

Coculture of 3T3-L1 adipocytes with RAW264.7 macrophages led to a larger number of small-sized lipid droplets suggesting that triglycerides were mobilized and secreted as FFAs (Figure 13G). The admixture of 30µM palmitate masked cocultural effects and resulted in a size of lipid droplets comparable to 3T3-L1 (Figure 13H). These findings suggest that 3T3-L1 adipocytes took up palmitate to store it in lipid droplets. Nevertheless, compared to 3T3-L1, lipid droplet size is reduced in coculture indicating lipolysis. The presence of 250µM palmitate resulted in a further enlargement of lipid droplets (Figure 13I), suggesting that 3T3-L1 adipocytes took up even more palmitate. Nonetheless, coculture reduced the lipid droplet size compared to 3T3-L1, suggesting triglyceride mobilization. Unfortunately it was not possible to monitor RAW264.7 macrophages under coculture conditions. The transwell membrane prevents microscopical observations, thus a definite statement concerning the condition of the RAW264.7 macrophages under cocultural conditions was not possible.

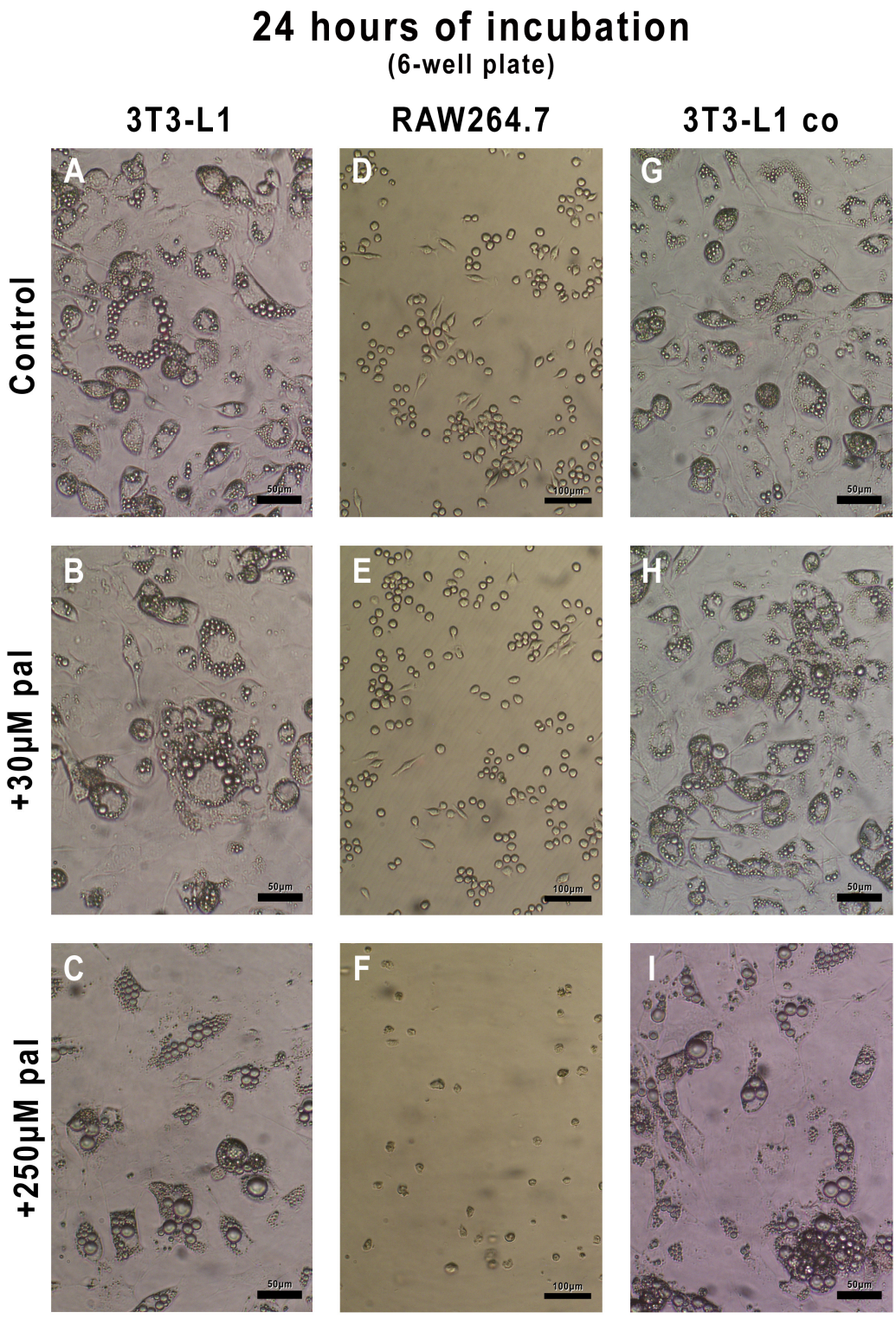

Figure 13: 3T3-L1 adipocytes (A–C), RAW264.7 macrophages (D–F) and 3T3-L1 adipocytes cocultured with RAW264.7 macrophages (G–I) after 24 hours of incubation in absence or presence of palmitate. co, coculture; pal, palmitate.

3.2.1.1. Tumor necrosis factor α quantification

Tumor necrosis factor α (TNFα) is a well-known marker of inflammation and increased in obese adipose tissue (12, 13). Moreover, macrophage deprived TNFα plays an important role in the induction of inflammatory changes in adipocytes (1). The TNFα concentration was measured in the supernatant of 3T3-L1 adipocytes, RAW264.7 macrophages and the coculture; results are depicted in Figure 14.

In the absence of palmitate, a time-depended increase in TNFα concentration can be observed for adipocytes, macrophages and the coculture (Figure 14A). In general the TNFα level is higher in RAW264.7 macrophages than in 3T3-L1 adipocytes. These results suggest that, in contrast to RAW264.7 macrophages, 3T3-L1 adipocytes do not secrete high amounts of TNFα. Therefore, the majority of TNFα is macrophage-deprived. Furthermore, RAW264.7 cells stimulate themselves under stress condition or at high desity to produce TNFα, which results in continuously increasing TNFα concentration (Figure 14).

In coculture, over time a continuous increase of the TNFα level can be observed. Nevertheless, the concentration is comparable to the one in RAW264.7 cells until 24 hours of incubation. These findings suggest that TNFα is induced in coculture but not as a result of adipocytes-macrophage communication since RAW264.7 macrophages appear to be a more likely source.

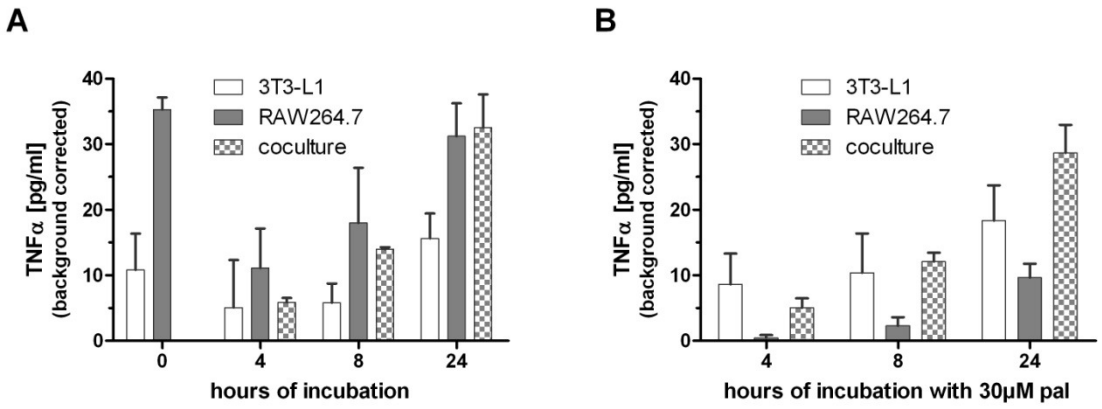

Figure 14: TNFα levels measured in supernatant of samples incubated without (A) or in presence of 30µM palmitate (B). pal , palmitate; error bars, S.D.; (n=3).

In the presence of palmitate, a time-dependent increase in TNFα is observed for adipocytes, macrophages and the coculture (Figure 14B). Compared to Figure 14A, macrophage TNFα concentration is markedly reduced, suggesting a beneficial effect of palmitate. This effect was not observed in the cytotoxicity assay and therefore remains unclear.

Under coculture conditions and in presence of palmitate, TNFα levels increase continuously over time, although slightly decreased compared to Figure 14A. These findings suggest that TNFα is induced in coculture as a result of adipocyte-macrophage communication, despite the self-stimulating effect of the macrophages.

3.2.1.2. Free fatty acid quantification

3T3-L1 adipocytes are known to secrete free fatty acids (FFAs), especially palmitate, e.g. under inflammatory conditions (1). It is thus important to monitor the FFA concentration in the supernatant, as FFAs activate inflammatory pathways in macrophages (1). The FFA concentration was measured in the supernatant of 3T3-L1 adipocytes, RAW264.7 macrophages and the coculture; results are depicted in Figure 15**.**

In 3T3-L1 adipocytes, an increased concentration of FFA can be observed after 4 hours before decreasing continuously (Figure 15A). These results suggest that 3T3-L1 cells took up FFAs in order to store them as triglycerides. For RAW264.7 macrophages and under coculture conditions, the FFA concentration is decreasing continuously, suggesting that FFAs are taken up. After 24 hours of incubation, FFA levels are almost comparable (Figure 15A). In compliance to Suganami, et al. (1), these findings suggest that under mentioned conditions, the interaction of adipocytes and macrophages is not sufficient to induce lipolysis.

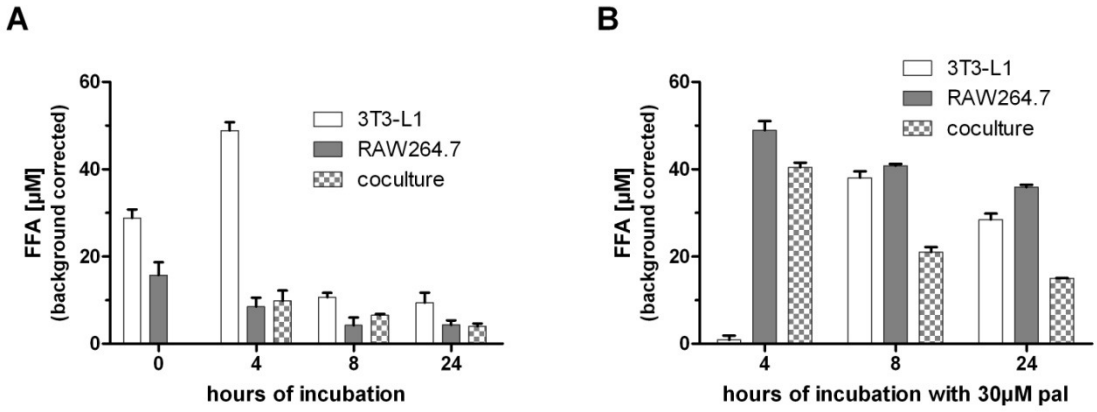

Figure 15: Measured free fatty acid (FFA) concentration of the supernatant without (A) or in presence of 30µM palmitate (B). pal, palmitate; error bars, S.D.; (n=3).

The addition of 30µM palmitate leads to changes in the FFA concentration (Figure 15B). For 3T3-L1 adipocytes the FFA concentration is considerably decreased after 4 hours, suggesting that 3T3-L1 cells took up FFAs in order to metabolize them. Nevertheless, the distinct increase after 8 hours of incubation is symptomatic of lipolytic processes. The reason for these contrary observations is currently unknown.

The time-dependent decrease of FFA concentration can be observed for both RAW264.7 macrophages and the coculture in presence of palmitate. After 24 hours, the FFA level is likewise for 3T3-L1 adipocytes and RAW264.7 macrophages, whereas it differs for the coculture (Figure 15B), indicating a coculture-specific effect.

3.2.1.3. Triglyceride quantification

Triglycerides (TGs) are a natural storage component of FFAs; in obese adipose tissue, triglyceride biosynthetic enzymes are decreased (36, 37). The development of the TG concentration was measured in the supernatant of 3T3-L1 adipocytes, RAW264.7 macrophages and the coculture in absence (Figure 16A) and presence of palmitate (Figure 16B).

The TG concentration for RAW264.7 macrophages is decreased after 4 hours of incubation and remains constant afterwards. These findings suggest that macrophages are not able to metabolize TGs. For 3T3-L1 adipocytes and coculture conditions, the TG concentration is increased after 24 hours of incubation (Figure 16A), suggesting an

enlarged secretion of TGs. The effects observed in coculture are most likely 3T3-L1-deprived indicating that under these conditions the cell-cell communication is not sufficient to induce visible effects. Therefore, the measured TG concentration is most likely adipocyte-deprived.

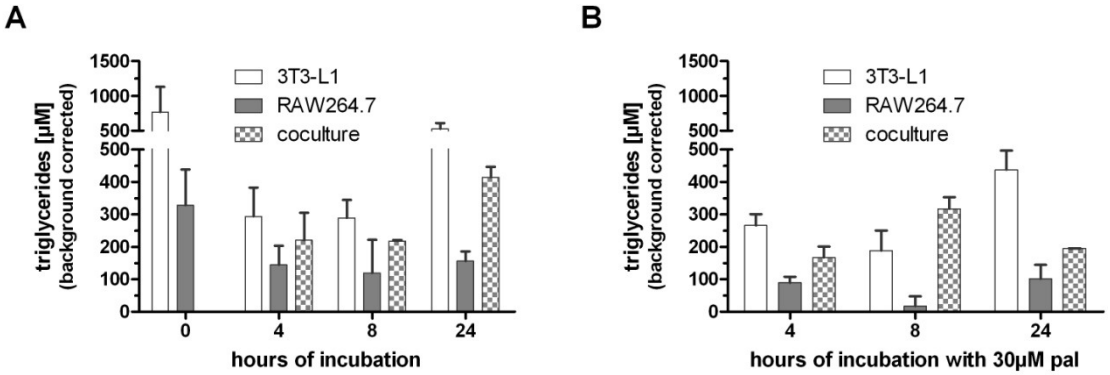

Figure 16: Measured triglyceride (TG) concentration of the supernatant without (A) or in presence of 30µM palmitate (B). pal , palmitate; error bars, S.D.; (n=3).

The addition of 30µM palmitate induces major changes in the TG level (Figure 16B). While the TG concentration remains constant for RAW264.7 macrophages, it slightly increases for 3T3-L1 adipocytes after 24 hours of incubation. These results suggest that RAW264.7 macrophages are unable to metabolize TGs, both in absence and presence of palmitate. Moreover, 3T3-L1 cells secrete TGs after 24 hours of incubation, independent of the presence of palmitate. In coculture, there is a distinguished peak after 8 hours of incubation (≈ 300µM TG). As already observed for the FFA concentration, the addition of 30µM palmitate leads to smaller TG concentrations compared to the values retrieved in absence of palmitate (Figure 16A). These findings suggest that in coculture, TG biosynthetic pathways are influenced leading to changes in TG concentration as monitored.

3.2.1.4. Induced changes on the mRNA level

The real-time polymerase chain reaction (real-time PCR) method was utilized to take a closer look at the expression level of cell markers (e.g. Adiponectin) or cyto- and chemokines (Tnfα, Mcp-1) of 3T3-L1 adipocytes and RAW264.7 macrophages.

Coculture

In general, single cell cultures of 3T3-L1 adipocytes and RAW264.7 macrophages were used as controls for cocultured cells. For cocultured 3T3-L1 adipocytes, the expression levels of the following genes were monitored: Adiponectin (Adipo), Fabp4, Mcp-1, Glut4, Resistin (Figure 17A).

While time-dependent changes are only of minor extent for Adiponectin, Resistin and Glut4, Fabp4 and Mcp-1 are influenced in a more apparent way. Fabp4 is expressed at a minimum after 8 hours of incubation, while Mcp-1 expression is increased 4-fold after 24 hours of incubation (Figure 17A). These findings suggest that expression of Mcp-1 is specifically up-regulated in coculture.

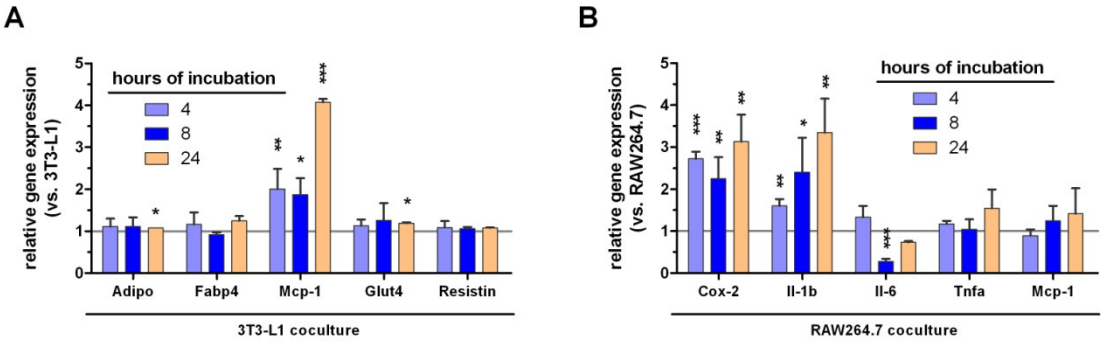

Figure 17: Relative gene expression for cocultured 3T3-L1 (A) and RAW264.7 (B). Adipo, Adiponectin; error bars, S.D.; *P<0.05, **P<0.01, ***P<0.001, (n=3).

For cocultured RAW264.7 macrophages, the expression levels of the following genes were monitored: Cox-2, Il-1b, Il-6, Tnfα and Mcp-1 (Figure 17B). In contrast to 3T3-L1 adipocytes, the time-dependent changes are more striking for RAW264.7 macrophages.

Expression of Il-1b and Mcp-1 is continuously increasing with incubation time, whereas the expression of Cox-2 and Il-6 is at a minimum after 8 hours, right before they increase (Figure 17B). These findings suggest that expression of Il-1b, Mcp-1 and TNFα is specifically up-regulated in coculture.

The expression pattern (after 24 hours of incubation) is slightly influenced by the addition of 30µM palmitate (Figure 18). In general, 3T3-L1 adipocytes are less impaired by palmitate than RAW264.7 macrophages. These results suggest that addition

of palmitate to cocultured 3T3-L1 cells does not induce considerable changes in the expression profile.

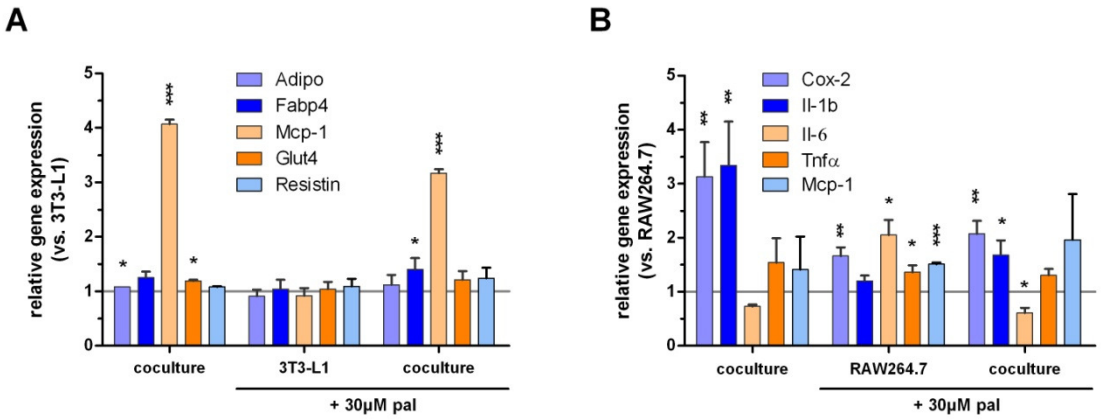

Figure 18: Relative gene expression for cocultured 3T3-L1 adipocytes (A) and RAW264.7 macrophages (B) in absence or presence of 30µM palmitate after 24 hours of incubation. Adipo, Adiponectin; pal, palmitate; error bars, S.D.; *P<0.05, **P<0.01, ***P<0.001, (n=3).

In cocultured RAW264.7 macrophages, addition of palmitate slightly reduced the gene expression (Figure 18B). Nevertheless, the expression pattern remained unchanged in presence of palmitate. These results suggest that the addition of 30µM palmitate did not aggravate the coculture-specific gene regulation.

Phosphorylation of peroxisome proliferator-activated receptor γ

Recently Choi, et al. (72) published a gene set comprising 17 genes regulated by the phosphorylation of peroxisome proliferator-activated receptor γ (PPARγ) at Ser273. Using Western Blot analysis, Choi, et al. (72) showed that phosphorylation of PPARγ in 3T3-L1 adipocytes can be induced by incubation with inflammation mediators such as IL-6 and TNFα, or FFA. As RAW264.7 macrophages produce high amounts of TNFα and IL-6 changes in the genes regulated by phosphorylation of PPARγ might be visible in cocultured 3T3-L1 adipocytes. This was investigated using real-time PCR. Results are plotted as a heat-map in Figure 19.

The development of the gene expression level for 3T3-L1 adipocytes incubated in presence of 30µM palmitate is illustrated in Figure 19A. After 4 hours of incubation, only Cyp2f2 is up-regulated, while Car3, Acyl, Rybp, Txnip and Nr1d1 remain unregulated. All remaining genes are down-regulated. When compared to the suggested

regulation (72), eight out of 17 genes match. After 8 hours of incubation, major changes in the expression level are visible; except for Rybp all genes are up-regulated. When compared to the suggested regulation (72), one out of 17 genes matches. In the end (after 24 hours), the majority of genes is unregulated except for Peg10 and Cd24a. These results suggest that PPARγ phosphorylation as a result of local adipose tissue inflammation reaches a maximum within the first 4 hours and decreases afterwards. Therefore palmitate addition led to an acceleration of the inflammatory phosphorylation process.

The development of the gene expression for cocultured 3T3-L1 adipocytes is illustrated in Figure 19B. After 4 hours of incubation, all genes are up-regulated. When compared to the suggested regulation (72), none of the genes match. After 8 hours of incubation minor changes in the expression level are visible. While Cyp2f2, Rarres2, Selenbp1 and Adipsin are down-regulated, Peg10, Cidec and Rybp remain unregulated. After 24 hours about half of the genes are down- or upregulated, whereas Acyl and Nr3c1 and Nr1d1 remain unregulated. When compared to the reported regulation (72), eight out of 17 genes match. These findings suggest that PPARγ phosphorylation is induced in coculture. Moreover, complete phosphorylation is not reached within 24 hours of incubation – and probably even later.

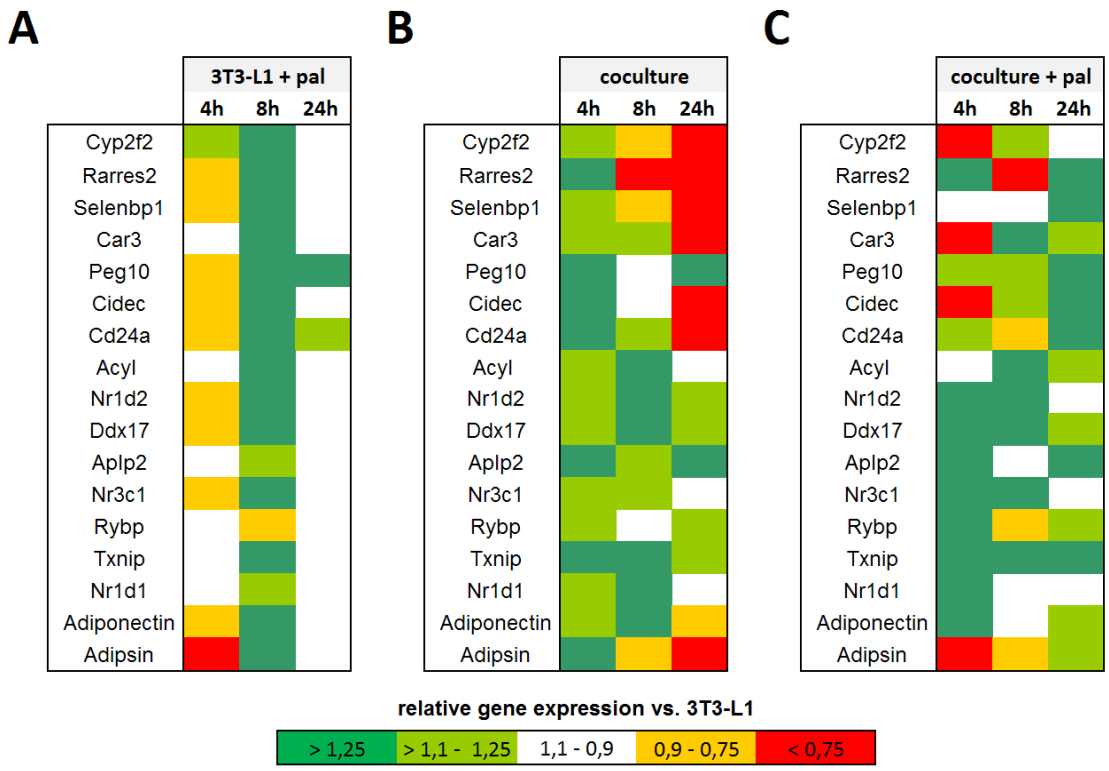

Figure 19: Heat-map of the relative expression of the gene set regulated by peroxisome proliferator-activated receptor γ (PPARγ) phosphorylation. The suggested gene set was tested for 3T3-L1 adipocytes incubated with 30µM palmiate (A), cocultured 3T3-L1 adipocytes (B) and cocultured 3T3-L1 adipocytes incubated with 30µM palmiate (C). pal, palmitate; (n=3)

The development of the gene expression level for cocultured 3T3-L1 adipocytes in presence of 30µM palmitate is illustrated in Figure 19C. After 4 hours of incubation only Cyp2f2, Car3, Cidec and Adipsin are down-regulated, while Selenbp1 and Acyl remain unregulated. All residual genes are up-regulated. When compared to the suggested regulation (72) five out of 17 genes match. After 8 hours of incubation minor changes in the expression level are visible. While Rarres2, Cd24a, Rybp and Adipsin are down-regulated, Selenbp1, Aplp2, Nr1d1 and Adiponectin remain unregulated. In the end (after 24 hours) the majority of genes is up-regulated while Cyp2f2, Nr1d2, Nr3c1 and Nr1d1 remain unregulated. In comparison to Choi, et al. (72), one out of 17 genes matches. These findings suggest that PPARγ phosphorylation is already decreasing after 4 hours of incubation; thus the phosphorylation is induced almost immediately. Hence, palmitate addition led to rapid acceleration of the phosphorylation process.

Palmitate-induced inflammation in RAW264.7 macrophages

Free fatty acids (FFAs) act as inducer of inflammation in RAW264.7 macrophages (1). The expression of several pro-inflammatory chemo- and cytokines as response to palmitate addition was measured using real-time PCR (Figure 20). Expression of all pro-inflammatory markers tested is increasing due to palmitate addition in a dose-dependent manner. Nevertheless, there is no distinct induction of TNFα expression until addition of 250µM palmitate (Figure 20C). In contrast, Il-1b and Il-6 (Figure 20A) and B) are already induced at 125µM palmitate and MCP-1 even at 30µM palmitate (Figure 20D). These findings suggest that palmitate induces inflammatory responses in macrophages in a dose-dependent manner.

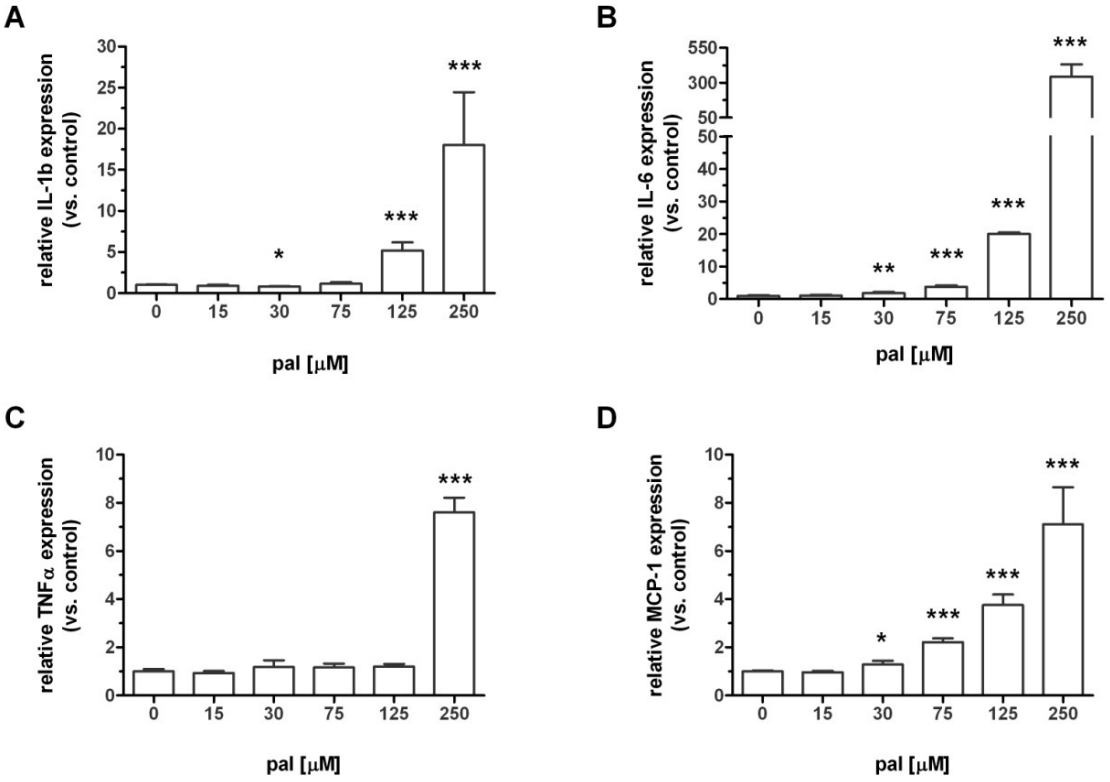

Figure 20: Palmitate induced gene expression of pro-inflammatory chemo- and cytokines in RAW264.7 macrophages. pal, palmitate; error bars, S.D.; *P<0.05, **P<0.01, ***P<0.001, (n=3).

The type II transmembrane c-type lectin Mincle, which is also known as macrophage-inducible C-type lectin, Clec4e or Clecsf9, is selectively induced in macrophages due to the interaction with adipocytes (50, 91). Furthermore, Matsumoto, et al. (92) identified Mincle as transcriptional target of the CCAAT/enhancer binding

protein β (CEBPβ), which is present in macrophages due to inflammatory stimuli. Recently Ichioka, et al. showed that the addition of palmitate induced Mincle mRNA expression in macrophages (50). To assess whether Mincle is a suitable marker of macrophage inflammation, the induction of mRNA expression after a 24h palmitate treatment was analyzed using real-time PCR. As depicted in Figure 21A, palmitate treatment resulted in a dose-dependent Mincle mRNA expression in RAW264.7 macrophages. Moreover, real-time PCR confirmed a highly selective mRNA expression of Mincle in RAW264.7 macrophages compared to 3T3-L1 adipocytes (Figure 21B). In addition, Mincle expression was up-regulated in RAW264.7 macrophages through addition of 75µM palmitate, coculture with 3T3-L1 adipocytes and the combination of both treatments (Figure 21A and C). These results suggest that Mincle is an appropriate macrophage-specific marker and is able to illuminate FFA-induced macrophage activation.

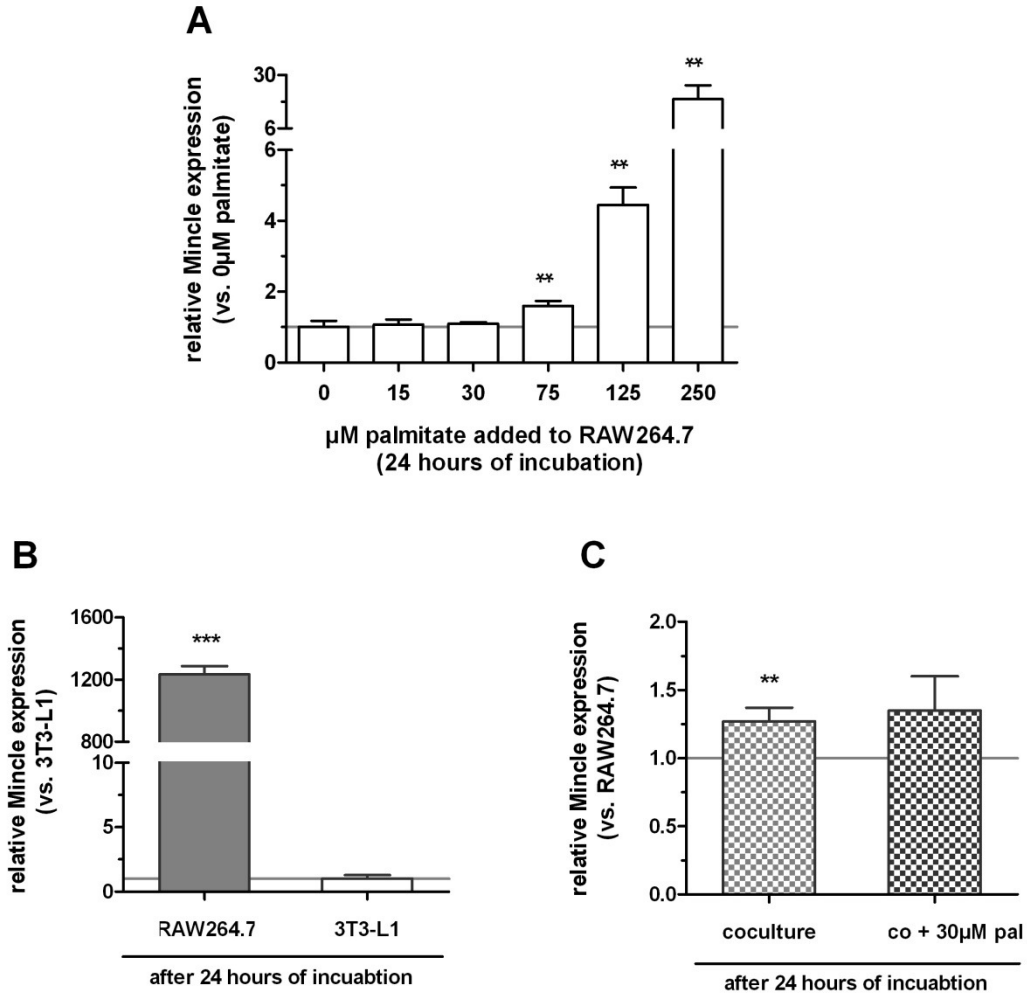

Figure 21: Mincle mRNA expression. (A) Palmitate induced expression of Mincle in RAW264.7 macrophages. (B) Selective expression of Mincle in RAW264.7 macrophages. (C) Expression of Mincle in RAW264.7 macrophages after 24 hours of coculture in absence or presence of 30µM palmitate. co, coculture; pal, palmitate; error bars, S.D.; *P<0.05, **P<0.01, ***P<0.001, (n=3).

3.2.2. Up-scaling of the coculture system for proteomics (50cm² dish)

Using the knowledge of the 6-well experiments, the coculture system was scaled up in order to study changes on the protein level. Due to the RNA-protein-delay and the results of the 6 well experiments, the incubation time was adapted. Hence, only the following incubation times were considered: 0 hours, 8hours and 24 hours. The conditions were studied by microscopy and by using already established biomarkers such as free fatty acid content, triglyceride concentration and tumor necrosis factor α amount. Moreover, protein was extracted in order to study coculture-induced changes by western blotting mass spectrometry.

Microscopical observations of RAW264.7 macrophages, 3T3-L1 adipocytes and cocultured 3T3-L1 adipocytes are depicted in Figure 22. All pictures were taken after 24 hours of incubation.

3T3-L1 adipocytes are characterized by numerous lipid droplets within each cell (Figure 22A). Coculture of 3T3-L1 adipocytes with RAW264.7 macrophages led to small-sized lipid droplets suggesting that triglycerides were mobilized and secreted as FFAs (Figure 22B). Moreover, compared to 3T3-L1, size and abundance of lipid droplets are of smaller scale in coculture, indicating lipolysis. These results are in agreement with the observations of the 6-well experiment.

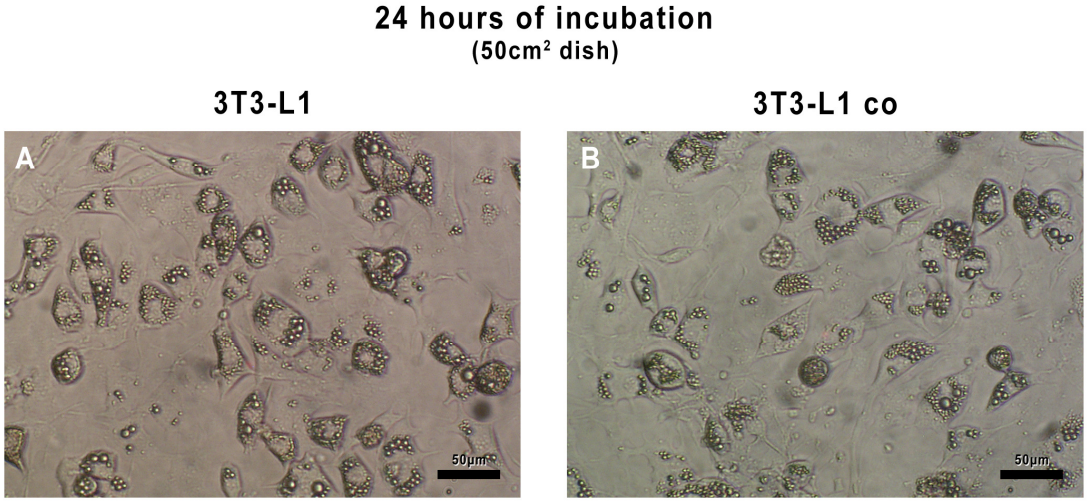

Figure 22: 3T3-L1 adipocytes (A) and 3T3-L1 adipocytes cocultured with RAW264.7 macrophages (B) after 24 hours of incubation. co, coculture.

3.2.2.1. Tumor necrosis factor α quantification

The tumor necrosis factor α (TNFα) concentration was measured in the supernatant of 25cm² flasks and 50cm² dishes. The flasks were used as controls, whereas dishes with transwell inserts were utilized for coculture experiments. For the larger dishes the incubation time was adapted, as 4 hours was too short to observe major changes on the protein level. Markedly coculture-induced are protein changes are expected after 24 hours of incubation.

The TNFα concentration in the flask (Figure 23A) remained unchanged for 3T3-L1 adipocytes. RAW264.7 cells stimulate themselves to produce TNFα which

results in a 3-fold increased TNFα concentration (Figure 23A). The TNFα concentration in coculture (Figure 23B) increased time-dependently. These findings suggest that TNFα is induced in coculture.

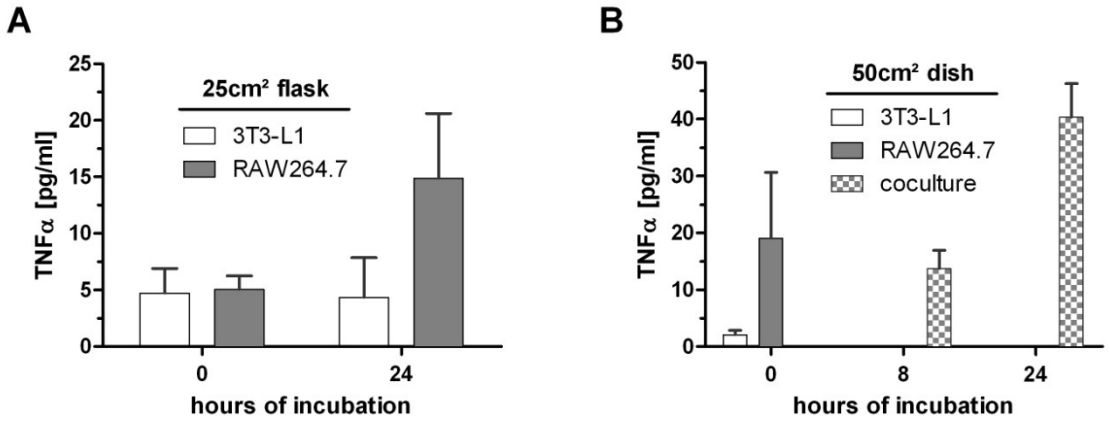

Figure 23: TNFα levels measured in the supernatant of flasks (A) or dishes (B). TNFα concentrations for RAW264.7 macrophages and coculture normalized to $1*10^6$ RAW264.7 macrophages seeded. Error bars, S.D.; (n=1-2).

3.2.2.2. Free fatty acid quantification

The free fatty acid (FFA) concentration was measured in the supernatant of 3T3-L1 adipocytes and RAW264.7 macrophages, which were cultured in a 25cm² flask. Furthermore, the FFA level was measured in the supernatant of the coculture. The flasks were used as controls, while the dishes were utilized for coculture experiments.

The FFA concentration in the flask (Figure 24A) decreased similarly in both cell lines after 24 hours of incubation, suggesting that both cell lines are capable of FFA metabolization. In coculture (Figure 24B), the FFA level remained unchanged until 24 hours of incubation. These results suggest that the free fatty acid uptake is abolished in coculture.

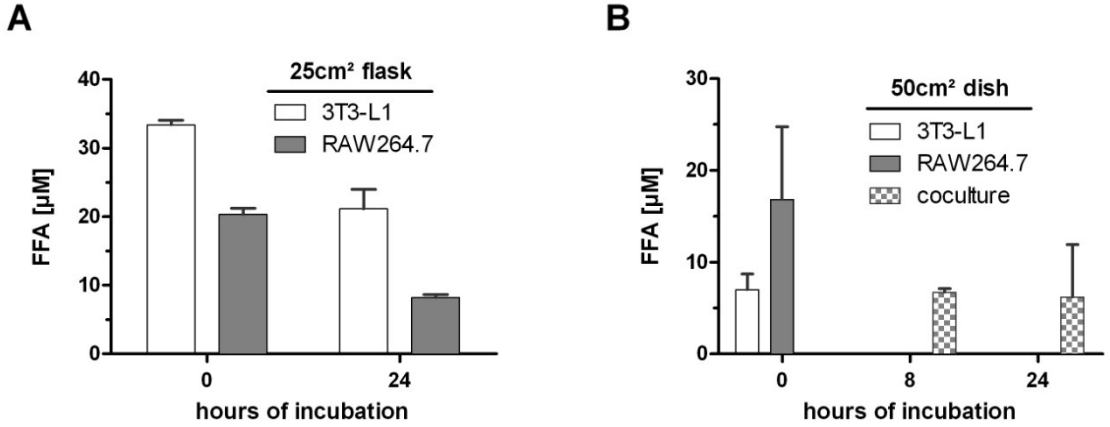

Figure 24: Free fatty acid (FFA) levels measured in the supernatant of flasks (A) or dishes (B). FFA concentrations for RAW264.7 macrophages and coculture normalized to $1*10^6$ RAW264.7 macrophages seeded. Error bars, S.D.; (n=1-2).

3.2.2.3. Triglyceride quantification

The triglyceride (TG) concentration was measured in the supernatant of the coculture. Furthermore, the TG level was measured in the supernatant of 3T3-L1 adipocytes and RAW264.7 macrophages, which were cultured in a 25cm² flask. The flasks were used as controls, while the dishes were utilized for coculture experiments.

The TG concentration in the flask (Figure 25A) decreased similarly in both cell lines, indicating that both cell lines are able to metabolize TGs. In the coculture (Figure 25B), the TG level did not increase markedly. The results for RAW264.7 macrophages and the coculture are contrary to those in the 6-well formats.

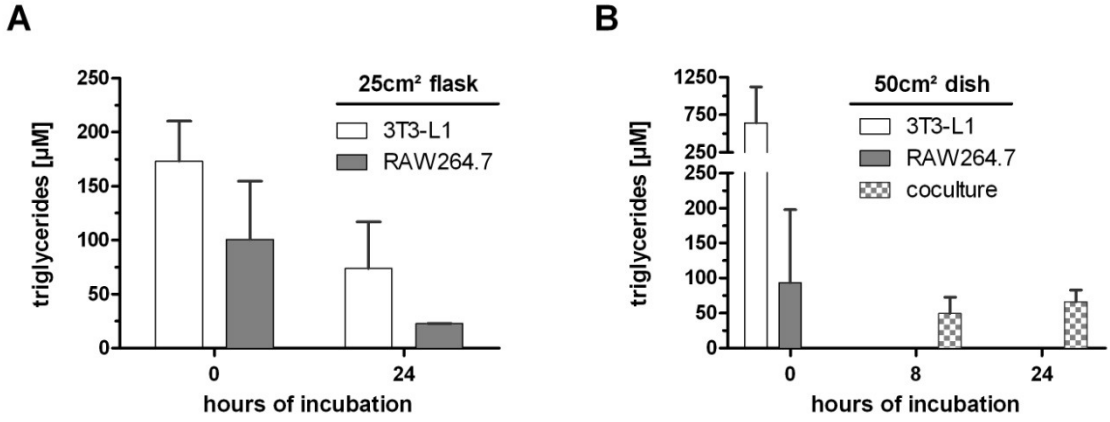

Figure 25: Triglyceride (TG) levels measured in the supernatant of flasks (A) or dishes (B). TG concentrations for RAW264.7 macrophages and coculture normalized to $1*10^6$ RAW264.7 macrophages seeded. Error bars, S.D.; (n=1-2).

3.2.2.4. Protein samples

Proteins were obtained from 50cm² dishes and in general isolated for proteomic analysis and western blotting.

Western blotting

Protein phosphorylation is a central modification used for cell regulation and signaling, thus, one out of three eukaryotic proteins is phosphorylated (93). Furthermore, phosphorylation is often utilized as a fast response to e.g. cellular stress (57-59). The phosphorylation state of JNK, cJun and IRS-1 were measured under cocultural conditions using western blotting.

JNK

JNK is a key participant of several signaling pathways such as inflammation, insulin signaling and endoplasmatic reticulum stress, and is commonly phosphorylated under stress conditions (8, 22, 40, 57, 61). Western blot analysis confirmed larger magnitudes of JNK in RAW264.7 macrophages compared to 3T3-L1 adipocytes. Thus, cocultured RAW264.7 macrophages were used instead of the 3T3-L1 adipocytes for monitoring the phosphorylation state.

The development of JNK phosphorylation is documented in Figure 26; results of the densitometric analyses are depicted in Figure 26B and Figure 26C. Coculture with 3T3-L1 adipocytes led to a continuous increase of JNK phosphorylation in RAW264.7 macrophages. After 24 hours of incubation, compared to its unphosphorylated counterpart, twice the amount of modified JNK was detected. Corresponding to these findings, the amount of JNK (compared to β-actin (Figure 26C)) is only slightly raised until 8 hours of incubation, before a roughly increase (≈1.5 fold) can be observed after 24 hours. This indicates that coculture of adipocytes and macrophages results in an increased JNK phosphorylation due to cellular stress.

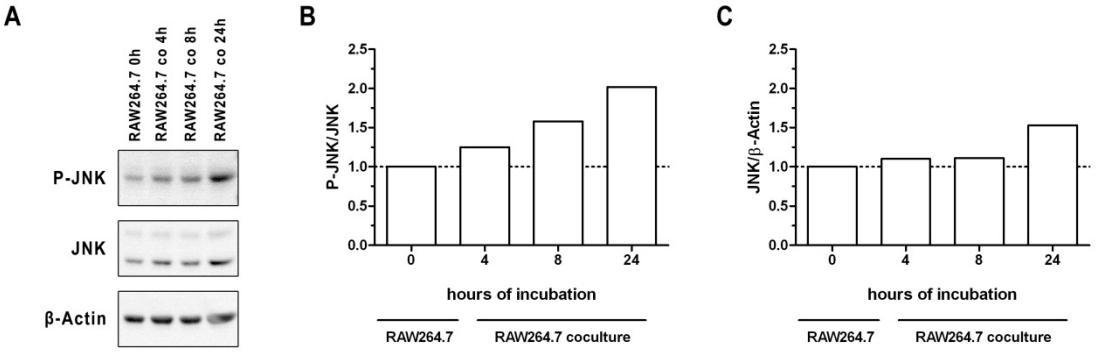

Figure 26: Induction of JNK phosphorylation under cocultural conditions. (A) Western blot analysis. (B-C) Densitometric analyses. (C) Relative amount of JNK. (n=1).

cJUN

As a downstream target of JNK, cJun gets phosphorylated under stress conditions (57). Western blot analysis confirmed large quantities of cJun in RAW264.7 macrophages compared to 3T3-L1 adipocytes. Hence, cocultured RAW264.7 macrophages were used instead of 3T3-L1 adipocytes in order to monitor the state of phosphorylation.

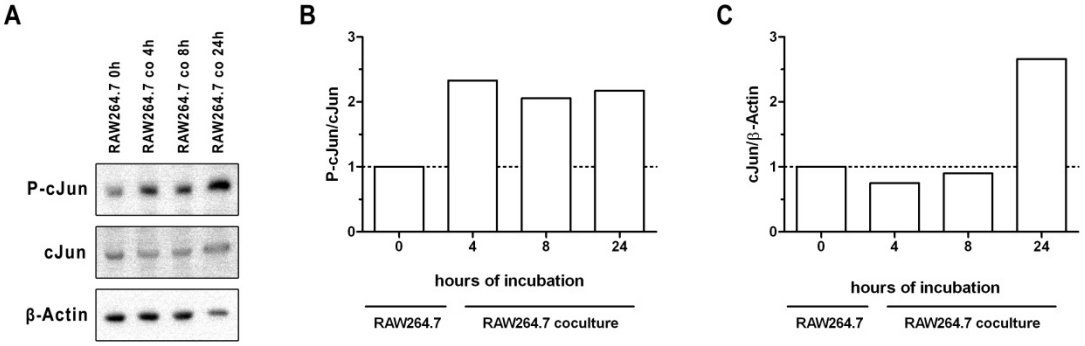

Figure 27: Induction of cJun phosphorylation under cocultural conditions. (A) Western blot analysis. (B-C) Densitometric analyses. (C) Relative amount of cJun. (n=1).

Figure 27 depicts the development of cJun phosphorylation and the results of the densitometric analyses (Figure 27B and C). Coculture with 3T3-L1 adipocytes led to an almost instant increase of cJun phosphorylation in RAW264.7 macrophages (≈2-fold). Moreover, the phosphorylation level remained constantly high under cocultural conditions. The amount of cJun (compared to β-actin (Figure 27C)) is only slightly regulated until 8 hours of incubation, before markedly increasing

after 24 hours (≈1.5 fold). This indicates that under cocultural conditions, cJun phosphorylation is induced.

IRS-1

IRS-1 is a key molecule in insulin signaling and impairs insulin signaling when phosphorylated at Ser307 (22, 23, 94). Western blot analysis confirmed large amounts of IRS-1 in 3T3-L1 adipocytes (data not shown). Due to the abundance of IRS-1 in adipocytes, cocultured 3T3-L1 adipocytes were used instead of to RAW264.7 macrophages to monitor the state of phosphorylation.

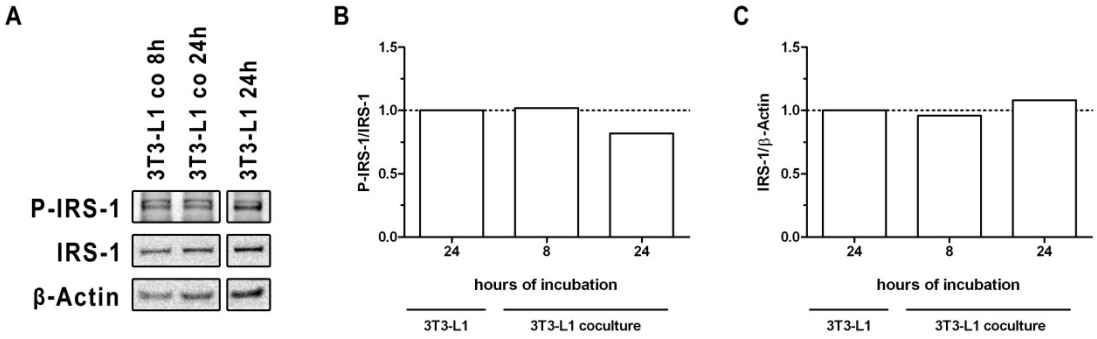

Figure 28: Induction of IRS-1 phosphorylation under cocultural conditions. (A) Western blot analysis. (B-C) Densitometric analyses. (C) Relative amount of IRS-1. (n=1).

The development of IRS-1 phosphorylation is documented in Figure 28; results of the densitometric analyses are depicted in Figure 28B and Figure 28C. Coculture with RAW264.7 macrophages did not increase IRS-1 phosphorylation (Figure 28B). Moreover, the amount of IRS-1 protein (compared to β-actin) is constant during the whole experiment (Figure 28C). These findings suggest that 24 hours of coculture are not sufficient to induce IRS-1 phosphorylation in the current coculture setup.

3.2.2.5. Mass spectrometry analysis

Analysis of in-gel digested samples

The in-gel digestion was performed for two reasons. At first to verify that the purified samples from the coculture dishes contained enough material for MS analysis and second to estimate whether a quantitative approach would be worthwhile. Therefore, all samples were run on a 10% SDS gel. Afterwards, 3 bands were cut out and an in-gel

digestion with trypsin was performed. The samples were analyzed using the LTQ Orbitrap XL. Results are summarized in Table 5.

sample		3T3-L1 24h	3T3-L1 co 24h	RAW 24h	RAW co 24h
gel slice	1	117	264	237	299
	2	224	362	370	424
	3	365	444	452	474
average		235	357	353	399

Table 5: Number of identified proteins per gel slice after in-gel digestion. (n=1).

These results indicate that a sufficient number of proteins can be identified. Moreover, a combination of coculture experiments with mass spectrometry is possible. In case of the 24 hours cultured 3T3-L1 adipocytes 235 proteins per gel slice were identified on an average. Since this was only a pilot experiment, with 3 slices cut out, a total of about 3760 identified proteins is expected under 'normal' conditions, where 16 slices are cut.

Due to space constraints, full protein lists are not included in this thesis. Therefore, only some of the identified proteins shall be mentioned in extracts.

For 3T3-L1 adipocytes only Cyp2f2, perilipin, Carnitine-O-palmitoyltransferase 1 and Lipoprotein lipase (LPL) shall be enlisted. Cytochrome oxydase P450 (Cyp2f2) is a member of the gene set regulated by PPARγ phosphorylation (72). While perilipin coats adipocyte lipid droplets, Carnitine-O-palmitoyltransferase 1 (CPT1) is a mitochondrial transferase enzyme responsible for the CoA import. Recentyl CTP1A was identified to attenuate FFA-induced insulin resistance and inflammation through JNK inhibition (95).

Lipoprotein lipase is a central enzyme of the glycerolipid metabolism and hydrolyzes triglycerides. Moreover, proteins belonging to the following pathways were identified: glycolysis metabolism, oxidative phosphorylation, tricarboxylic acid cycle and glycerolipid metabolism.

For RAW264.7 macrophages, TLR2 shall be mentioned which functions, similar to TLR4, as FFA sensor. Moreover, proteins belonging to the following pathways were

identified: oxidative phosphorylation, tricarboxylic acid cycle and pentose phosphate pathway.

These findings suggest that a quantitative approach is worthwhile, since in the three analyzed slices numerous proteins were identified. Moreover, several references to metabolic pathways and coculture-induced changes were gained.

Analysis of the SILAC quantification

The SILAC approach was used as pilot experiment to assess the applicability of SILAC-labeling and coculture experiments. Thus, all samples were reduced, alkylated and digested before purification with a C18 Tip. Finally, the samples were mixed at a 1:1 ratio with the corresponding standard and were analyzed using the LTQ Orbitrap XL.

Due to the small overlap between sample and SILAC-standard, a quantitative analysis was impossible for 3T3-L1 adipocytes (data not shown). However, some results (ratio of ratios) could be gained for RAW264.7 macrophages All three enzymes regulated are part of the glycolysis. Phosphoglycerate kinase is a transfer enzyme, responsible for ATP generation while the pyruvate kinase isoenzyme utilizes ATP to generate phosphoenolpyruvate (PEP).

	RAW co 8h	RAW co 24h
Phosphoglycerate kinase 1	2,26	1,03
	RAW co 8h	**RAW co 32h**
Triosephosphate isomerase	4,63	1,20
	RAW co 8h	**RAW 24h**
Pyruvate kinase isozymes M1/M2	1,39	0,61

ratio of ratios
< 0.8
< 0.5
> 1.5
> 1.2

Figure 29: Quantitative analysis of SILAC-labeled samples. (n=1).

All three glycolytic enzymes were markedly up-regulated after 8 hours of coculture suggesting an up-regulation of glycolysis. Although in this pilot experiment quantitative analysis was possible only for a few identified proteins, these finding suggest that the spike-in SILAC technique is practicable using the system set up introduced in this thesis.

4. Discussion

4.1. FFA induced cytotxicity

In the cytotoxicity assay, a reduction of RAW264.7 viability was observed due to palmitate addition (Figure 11A). The palmitate concentration, where the viability is reduced to 90% was determined with 30.65 ± 1.04µM palmitate. This level is quite low, considering the circumstance that in some publications, RAW264.7 macrophages were treated with up to 500µM palmitate (1, 41, 48, 96). Nevertheless, in order to amplify cocultural effects a maximum of 30µM palmitate was added. The amount of palmitate is enough to induce an inflammatory response in RAW264.7 macrophages without a significant reduction of viability. The findings of the cytotoxicity assay are in agreement with microscopic observations depicted in Figure 12. The addition of 30µM palmitate to RAW264.7 macrophages did not influence the optical conditions of the cells, although the cell number was reduced. Therefore, 30µM palmitate is sufficient to slightly disturb RAW264.7 metabolism without inducing a massive stress response.

4.2. Cocultural effects

The 6-well plate was used as a small-scale system for coculture experiments to evaluate changes on the RNA level. In coculture, lipolysis could only be detected microscopically but not via FFA quantification. Moreover, an increase of TNFα concentration and a palmitate-influenced TG metabolism was observed. Summarizing the 6-well plate works fine as a starting system and is easier to handle when checking different conditions and time points using biological replicates. Furthermore, it provides useful insights for the design of the dish coculture system.

The 50cm² dishes were used as an up-scaled coculture system, to determine coculture-induced changes of the proteasome. Due to being a large-scale version of the 6-well setup, all previously mentioned remain valid. With the help of the 6-well experiments, time points could be determined where coculture-induced changes are detectable. In contrast to its 6-well pendant, the larger dishes enable us to culture enough cells for protein extraction. Overall, the 50cm² dish system appears to be less

susceptible and more stable than the 6-well plate system, which is why I am recommending it for further investigations.

4.2.1.1. Microscopical observations in coculture systems

Unfortunately, it was impossible to observe cocultured RAW264.7 macrophages microscopically. After being seeded into the transwell insert, the cells are more or less indiscernible. Hence, coculture-induced changes have to be monitored in cocultured 3T3-L1 adipocytes (Figure 13G – I, Figure 22B). An alternative would be to switch cell lines, such as 3T3-L1 being cultured in the insert while RAW264.7 being seeded into the bottom of the well.

In the small-scale system (6-well plate) 3T3-L1 adipocytes took up palmitate and stored it in form of triglycerides in their lipid droplets (Figure 13B and 13C). 3T3-L1 adipocytes seem to be able to handle even very high palmitate concentrations (Figure 13C). Cocultured 3T3-L1 adipocytes depicted a reduced lipid droplet size even in presence of 30µM palmitate, suggesting free fatty acid secretion and lipolysis (Figure 13G and 13H, Figure 22B). Thus coculture of adipocytes and macrophages induced lipolysis in adipocytes. Therefore an increase in free fatty acid concentration should be measurable. Although the addition of palmitate seems to compensate lipolytic processes at least to a certain extent, palmitate does not circumvent lipolysis. These observations support recent publications of a paracrine loop between adipocytes and macrophages and coculture-induced lipolysis (1).

4.2.1.2. Coculture-induced increase of TNFα concentration

Although the majority of TNFα is macrophage-deprived (1), 3T3-L1 adipocytes are capable of TNFα secretion as well (Figure 14, Figure 23).

In both coculture systems, TNFα is continuously increasing (Figure 14A, Figure 23A), indicating that TNFα production is increasing in RAW264.7 macrophages under cocultural conditions (1). One reason for TNFα induction might be the inert ability of RAW264.7 macrophages to produce TNFα triggered by confluence stimuli. Nevertheless, the significant increase after 24 hours of incubation is most likely

coculture-induced. Hence, coculture of RAW264.7 macrophages and 3T3-L1 adipocytes led to an increased TNFα level.

In the small scale system, the addition of 30µM palmitate points out the coculture-specific TNFα induction (Figure 14B). Moreover palmitate addition reduced the TNFα concentration in RAW264.7 supernatant, suggesting a reduction of inflammatory responses. These observations indicate a beneficial impact of palmitate on macrophages and corresponding to Paracelsus' prediction: 'Dosis sola venenum facit'. Nevertheless, an advantageous effect of palmitate was not observed in the cytotoxicity assay. Therefore the main cause for a reduced TNFα production in RAW264.7 cells remains currently unknown. In agreement to the microscopic observations, addition of palmitate did not influence 3T3-L1 adipocytes (Figure 14B). These results reinforce the important role of TNFα in the communication of adipocytes and macrophages (1). Furthermore, free fatty acid addition seems to be necessary in order to guarantee obesity-like conditions.

4.2.1.3. Free fatty acid concentration

In both culture systems, adipocytes and macrophages were capable to metabolize FFAs (Figure 15A, Figure 24A). Furthermore, in small-scale coculture the FFA content was decreasing time-dependently, whereas in the large-scale coculture the FFA content was constant over 24 hours. These findings prefigure lipogenesis for 3T3-L1 adipocytes and RAW264.7 macrophages. Nevertheless, lipolysis is the expected metabolic pathway, especially under cocultural conditions.

Even in the presence of 30µM palmitate, FFAs are taken up and metabolized in RAW264.7 macrophages and coculture. 3T3-L1 adipocytes absorbed almost all FFAs before secreting them after 8 hours of incubation (Figure 15B), suggesting lipolytic events between 4 and 8 hours of incubation. Hence, lipolysis was induced due to limited storage capacities and an overstimulation of the hormone sensitive lipase (97). Hormone sensitive Lipase is the enzyme responsible for the convertion of triglycerides to FFAs in adipose tissue. The overstimulation leads to an immense FFA release Figure 15B) which marks the initial event of lipid deposition in non-adipose tissue (97).

nomenclature	GPR43 (FFAR2)	GPR41 (FFAR3	GPR120
Natural agonist (FFA)	short C2 – C4	Short C2 – C4	Medium C10 – C22
expression	Adipose tissue	Adipose tissue	Macrophages

Table 6: FFA receptors (adapted from Hara, et al. (98))

An early response mechanism of macrophages to FFAs involves lipid-handling mechanisms including storage in lipid droplets, β-oxidation and cholesterol efflux (97). Nuclear receptors peroxisome, proliferator-activated receptors (PPARs) and fatty acid binding proteins (FABPs) are known to function as sensors for FFAs. Furthermore free fatty acid receptors (FFARs) have been indentified in macrophages (GPR120) and adipocytes (GPR43, GPR41) (98). A short overview is given in Table 6. A chronic lipid exposure results in the collapse of these lipid-handling mechanisms and induction of lipotoxic events, such as disproportionate secretion of pro-inflammatory cytokines and cell death (97). Probably, 3T3-L1 cells did not secrete enough FFAs and 30µM palmiate are not considered as a signal of danger for macrophages. Due to the missing free fatty acid feedback, the vicious cycle was intercepted, thus lipolytic events are not visible.

Furthermore the microscopically observed lipolysis could not be confirmed by the FFA quantification assay. Obviously the paracrine loop between adipocytes and macrophages is not sufficient to induce FFAs secretion in 3T3-L1 cells. Lipolysis is observed in neither of the coculture systems.

4.2.1.4. Triglyceride concentration

In the small-scale system, RAW264.7 macrophages in contrast to 3T3-L1 adipocytes seem to unable to metabolize TGs (Figure 16A). In coculture and for 3T3-L1 adipocytes TG concentration markedly increases after 24 hours of incubation. These observations suggest that the increased TG level is likely to be attributed to 3T3-L1 deprivation rather than a cocultural effect. Under normal conditions 3T3-L1 convert TGs into FFAs which are taken up. Obviously the TG storage limit is reached after 24 hours in 3T3-L1 cells and in coculture. In the presence of palmitate, the TG profile remains unchanged for 3T3-L1 adipocytes and RAW264.7 macrophages (Figure 16B). In

coculture, palmitate addition led to a peak in TG concentration after 8 hours of incubation suggesting metabolic changes induced by coculture. The exact reasons for the observed TG changes remain unknown.

In the up-scale system, RAW264.7 macrophages and 3T3-L1 adipocytes were able to metabolize TGs, whereas in coculture the TG concentration remains unchanged (Figure 25). These observations suggest that TG uptake was inhibited in coculture. Furthermore, another reason could be a decreased expression of triglyceride biosynthetic enzymes due to coculture-induced inflammatory changes (36, 37).

4.2.1.5. Gene expression

In general, single cell cultures of 3T3-L1 adipocytes and RAW264.7 macrophages were used as controls for cocultured cells. For cocultured 3T3-L1 adipocytes, the expression levels of the following genes were monitored: Adiponectin (Adipo), Fabp4, Mcp-1, Glut4, Resistin (Figure 17A). In obese adipose tissue Adiponectin and Glut4 are down-regulated while Fabp4, Mcp-1 and Resistin are up-regulated (1, 72). Under cocultural conditions, this regulation could only be noticed for Mcp-1. These observations suggest that RAW264.7 macrophages are only partly able to induce inflammatory changes in 3T3-L1 cells. For cocultured RAW264.7 macrophages, the expression levels of the following genes were monitored: Cox-2, Il-1b, Il-6, Tnfα and Mcp-1 (Figure 17B). In obese adipose tissue, pro-inflammatory macrophage markers are up-regulated due to the chronic low-grade inflammatory state (Figure 20). Under cocultural conditions, this regulation is true for almost all markers, except for IL-6 which is down-regulated after 24 hours. These findings indicate that coculture with 3T3-L1 adipocytes induce inflammatory changes in RAW264.7 cells. In general Mcp-1 expression is increased further in cocultured 3T3-L1 cells rather than in cocultured RAW264.7 macrophages (1).

The addition of 30µM palmitate decreases the expression fold but not the expression profile (Figure 18). Therefore, palmitate, at least at the concentration tested, is not able to aggravate inflammatory conditions in both cell lines.

PPARγ phosphorylation

Choi, et al. (72) identified a gene cluster of 17 genes to be regulated depending on the phosphorylation of PPARγ at Ser273. Some of these genes were sorted according to their function as depicted in Figure 30.

According to Choi, et al. (72), PPARγ phosphorylation is induced in 3T3-L1 adipocytes in presence of palmitate and in cocultured 3T3-L1 adipocytes (in absence and presence of palmitate). While for cocultured 3T3-L1 adipocytes the maximum high point was already passed after 4 hours of incubation in presence of 30µM palmitate. In absence of palmitate, it was not reached within 24 hours of incubation (Figure 18B and 17C). These observations suggest that coculture induced phosphorylation of PPARγ. Moreover, in the absence of palmitate, incubation time should be extended in order to guarantee phosphorylation. The addition of palmitate markedly accelerated the phosphorylation process. Genes regulated by differential PPARγ phosphorylation are clustered according to their function in Figure 30. Nevertheless, gene expression clusters observed in qPCR are not related to the function of the gen.

receptors
retinoic acid receptor responder (Rarres2)
nuclear receptor (Nr1d2, Nr3c1, Nr1d1)

binding proteins
selenium binding protein 1 (Selenbp1)
RING1 and YY1 binding protein (Rybp)

lipid droplet formation
cell death-inducing DFFA-like effector c (Cidec)

interacting proteins
thioredoxin interacting protein (Txnip)

immune components
cluster of differentiation 24 antigen (Cd24a)
complement factor D (Adipsin)

glucose homeostasis
amyloid beta (A4) precursor-like protein 2 (Aplp2)
Adioponectin

enzymes
cytochrome P450 family (Cyp2f2)
carbonic anhydrase (Car3)
RNA helicase (Ddx17)

Figure 30: Members of the gene set regulated by PPARγ phosphorylation at Ser273.

Mincle as macrophage-specific marker of FFA-induced inflammation

Mincle is up-regulated in a dose-dependent manner for palmitate concentrations exceeding 75µM (Figure 21A). Moreover it is specifically expressed in RAW264.7 macrophages and increasingly expressed in coculture (Figure 21B and 21C). These findings are in agreement with recently published data (50). Due to the linkage of expression fold to FFA content, Mincle expression was compared to TNFα, the inflammatory marker in RAW264.7 macrophages. Furthermore, TNFα was identified as member of the paracrine loop comprising FFA.

The expression level in macrophages is comparable for both genes at small palmitate concentrations (0 – 30µM). Nevertheless, Mincle proved to be more sensible at palmitate levels exceeding 30µM (Figure 31A). However, under cocultural conditions the differences are more obvious. Although the general course of regulation is identical, the degree of is slightly diverse (Figure 31B). Due to the specific expression mechanism, Mincle might be the more suitable marker for cocultural effects. Nevertheless, Mincle is a newly identified target and therefore much remains to be unknown. Hence, I recommend the use of both markers, TNFα and Mincle in order to analyse coculture effects.

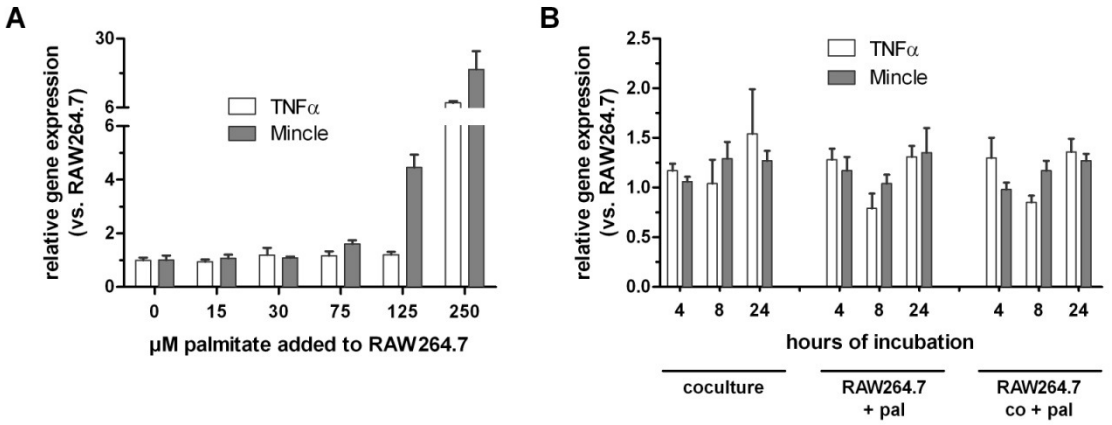

Figure 31: Comparison of Mincle and TNFα expression levels. (A) Expression of Mincle and TNFα in RAW264.7 macrophages incubated in presence of palmitate for 24 hours. (B) Expression of Mincle and TNFα in coculture and RAW264.7 macrophages in absence and presence of palmitate. co, Coculture; pal, palmitate; error bars, S.D.; (n=3).

4.2.1.6. Western blots

In order to determine the optimal time point for maximal changes on protein level, western blots were done. Moreover, characteristic targets of cellular stress (JNK, cJun) were utilized to determine coculture effects.

JNK and cJun

In coculture, a time-depended increase of JNK phosphorylation was observed (Figure 26). As phosphorylation of JNK is induced by inflammatory cytokines, FFAs, ER stress or hyperlipidemia (8, 22, 40, 57, 61), these findings suggest that the interaction between 3T3-L1 adipocytes and RAW264.7 macrophages is sufficient to induce inflammatory changes. Moreover, increased JNK activation is linked to the inhibitory phosphorylation of IRS-1 at Ser307 (58), indicating that an increased IRS-1 phosphorylation might be induced and even visible in coculture.

As a downstream target of JNK, cJun phosphorylation should increase in coculture. Anyhow, phosphorylation of cJun was induced almost instantly in coculture (Figure 27). These findings are in agreement with recently published data (57).

IRS-1

IRS-1 is a key player in insulin resistance. An increased JNK activation is linked to the inhibitory phosphorylation of IRS-1 at Ser307 (58). Nevertheless, there was no induction of IRS-1 phosphorylation during 24 hours of coculture (Figure 28). These findings indicate that phosphorylation of IRS-1 might take longer as IRS-1 is not a primary target of JNK. Moreover, the termination of insulin signaling due to IRS-1 phosphorylation at Ser307 results would induce major changes in various signaling pathways. Hence, 24 hours of coculture might not be long enough to induce such severe reactions.

4.2.1.7. Mass spectrometry analysis

In-gel digested samples

Numerous proteins, including several indicator proteins, could be identified. Extrapolating the findings of this experiment, a total of about 3,500 proteins is expected

to be identified, when processing 16 gel slices of a SDS-Page. The up-scale coculture system provides enough material for mass spectrometry analysis and the high protein amount, indicate that a quantitative approach will be the next step.

SILAC quantification

Results (ratio of ratios) could only be gained for RAW264.7 macrophages (Figure 29). All three enzymes are part of the glycolysis and were markedly up-regulated after 8 hours of coculture. This pilot experiment verified, that the spike-in SILAC technique can be combined with the coculture system set up in this thesis. Although western blotting suggested major changes at the protein level to be happening after 24 hours of incubation, major impacts in glycolytic enzymes were observed earlier. This observation emphasizes the necessity and advantage of a quantitative proteomics using mass spectrometry.

4.3. Outlook

Further assignment is needed to determine factors mediating the adipocyte-macrophage communication. This will be done by confirming the findings from the 50cm² dishes. Therefore, mRNA and protein extraction need to be done in larger (50cm²) dishes. For proteomic analysis, 24 hours of incubation seem to be the best choice, as several coculture-induced effects could be observed.

Moreover, the phosphorylation of PPARγ at Ser273 already observed on mRNA level has to be verified by western blotting. Besides, the findings concerning phosphorylation states for JNK and cJun have to be confirmed. Since IRS-1 phosporylation was not induced after 24 hours of cocultural incubation, an extended time frame would be necessary.

Since spike-in SILAC proved to be worthwhile, further work should focus on mass spectrometric analysis. Thus, the purification and extraction protocol has to be adapted and the overlap between sample and spike-in standard has to be looked into.

In order to understand mechanisms of cell regulation, it is important to examine posttranslational modifications, which control many biological processes. Mass spectrometry provides the opportunity to map and quantify changes in covalent modifications (99).

5. Indices

5.1. References

1. Suganami, T., Nishida, J., and Ogawa, Y. 2005. A paracrine loop between adipocytes and macrophages aggravates inflammatory changes - Role of free fatty acids and tumor necrosis factor alpha. *Arteriosclerosis Thrombosis and Vascular Biology* 25:2062-2068.
2. Keuper, M., Bluher, M., Schon, M.R., Moller, P., Dzyakanchuk, A., Amrein, K., Debatin, K.M., Wabitsch, M., and Fischer-Posovszky, P. 2011. An inflammatory micro-environment promotes human adipocyte apoptosis. *Mol Cell Endocrinol* 339:105-113.
3. Schenk, S., Saberi, M., and Olefsky, J.M. 2008. Insulin sensitivity: modulation by nutrients and inflammation. *J Clin Invest* 118:2992-3002.
4. Berg, A.H., and Scherer, P.E. 2005. Adipose tissue, inflammation, and cardiovascular disease. *Circ Res* 96:939-949.
5. Hotamisligil, G.S. 2006. Inflammation and metabolic disorders. *Nature* 444:860-867.
6. Pittas, A.G., Joseph, N.A., and Greenberg, A.S. 2004. Adipocytokines and insulin resistance. *J Clin Endocrinol Metab* 89:447-452.
7. Shoelson, S.E., Lee, J., and Goldfine, A.B. 2006. Inflammation and insulin resistance. *J Clin Invest* 116:1793-1801.
8. Wellen, K.E., and Hotamisligil, G.S. 2005. Inflammation, stress, and diabetes. *J Clin Invest* 115:1111-1119.
9. Itoh, M., Suganami, T., Hachiya, R., and Ogawa, Y. 2011. Adipose tissue remodeling as homeostatic inflammation. *Int J Inflam* 2011:720926.
10. Medzhitov, R. 2008. Origin and physiological roles of inflammation. *Nature* 454:428-435.
11. Nishimura, S., Manabe, I., Nagasaki, M., Hosoya, Y., Yamashita, H., Fujita, H., Ohsugi, M., Tobe, K., Kadowaki, T., Nagai, R., et al. 2007. Adipogenesis in obesity requires close interplay between differentiating adipocytes, stromal cells, and blood vessels. *Diabetes* 56:1517-1526.

12. Weisberg, S.P., McCann, D., Desai, M., Rosenbaum, M., Leibel, R.L., and Ferrante, A.W., Jr. 2003. Obesity is associated with macrophage accumulation in adipose tissue. *J Clin Invest* 112:1796-1808.

13. Xu, H., Barnes, G.T., Yang, Q., Tan, G., Yang, D., Chou, C.J., Sole, J., Nichols, A., Ross, J.S., Tartaglia, L.A., et al. 2003. Chronic inflammation in fat plays a crucial role in the development of obesity-related insulin resistance. *J Clin Invest* 112:1821-1830.

14. Clement, K., Viguerie, N., Poitou, C., Carette, C., Pelloux, V., Curat, C.A., Sicard, A., Rome, S., Benis, A., Zucker, J.D., et al. 2004. Weight loss regulates inflammation-related genes in white adipose tissue of obese subjects. *FASEB J* 18:1657-1669.

15. Hirai, S., Uemura, T., Mizoguchi, N., Lee, J.Y., Taketani, K., Nakano, Y., Hoshino, S., Tsuge, N., Narukami, T., Yu, R., et al. 2010. Diosgenin attenuates inflammatory changes in the interaction between adipocytes and macrophages. *Mol Nutr Food Res* 54:797-804.

16. Suganami, T., and Ogawa, Y. 2010. Adipose tissue macrophages: their role in adipose tissue remodeling. *Journal of Leukocyte Biology* 88:33-39.

17. Fantuzzi, G. 2005. Adipose tissue, adipokines, and inflammation. *J Allergy Clin Immunol* 115:911-919; quiz 920.

18. Attie, A.D., and Scherer, P.E. 2009. Adipocyte metabolism and obesity. *J Lipid Res* 50 Suppl:S395-399.

19. Mohamed-Ali, V., Pinkney, J.H., and Coppack, S.W. 1998. Adipose tissue as an endocrine and paracrine organ. *International Journal of Obesity* 22:1145-1158.

20. Saltiel, A.R., and Kahn, C.R. 2001. Insulin signalling and the regulation of glucose and lipid metabolism. *Nature* 414:799-806.

21. Reaven, G.M. 2005. The insulin resistance syndrome: definition and dietary approaches to treatment. *Annu Rev Nutr* 25:391-406.

22. Aguirre, V., Uchida, T., Yenush, L., Davis, R., and White, M.F. 2000. The c-Jun NH(2)-terminal kinase promotes insulin resistance during association with insulin receptor substrate-1 and phosphorylation of Ser(307). *J Biol Chem* 275:9047-9054.

23. Gual, P., Le Marchand-Brustel, Y., and Tanti, J.F. 2005. Positive and negative regulation of insulin signaling through IRS-1 phosphorylation. *Biochimie* 87:99-109.

24. Aguirre, V., Werner, E.D., Giraud, J., Lee, Y.H., Shoelson, S.E., and White, M.F. 2002. Phosphorylation of Ser307 in insulin receptor substrate-1 blocks interactions with the insulin receptor and inhibits insulin action. *J Biol Chem* 277:1531-1537.

25. Wellen, K.E., and Hotamisligil, G.S. 2003. Obesity-induced inflammatory changes in adipose tissue. *J Clin Invest* 112:1785-1788.

26. Yamauchi, T., Kamon, J., Waki, H., Terauchi, Y., Kubota, N., Hara, K., Mori, Y., Ide, T., Murakami, K., Tsuboyama-Kasaoka, N., et al. 2001. The fat-derived hormone adiponectin reverses insulin resistance associated with both lipoatrophy and obesity. *Nat Med* 7:941-946.

27. Maeda, N., Shimomura, I., Kishida, K., Nishizawa, H., Matsuda, M., Nagaretani, H., Furuyama, N., Kondo, H., Takahashi, M., Arita, Y., et al. 2002. Diet-induced insulin resistance in mice lacking adiponectin/ACRP30. *Nat Med* 8:731-737.

28. Diez, J.J., and Iglesias, P. 2003. The role of the novel adipocyte-derived hormone adiponectin in human disease. *Eur J Endocrinol* 148:293-300.

29. Steppan, C.M., Bailey, S.T., Bhat, S., Brown, E.J., Banerjee, R.R., Wright, C.M., Patel, H.R., Ahima, R.S., and Lazar, M.A. 2001. The hormone resistin links obesity to diabetes. *Nature* 409:307-312.

30. Muse, E.D., Obici, S., Bhanot, S., Monia, B.P., McKay, R.A., Rajala, M.W., Scherer, P.E., and Rossetti, L. 2004. Role of resistin in diet-induced hepatic insulin resistance. *J Clin Invest* 114:232-239.

31. Lu, S.C., Shieh, W.Y., Chen, C.Y., Hsu, S.C., and Chen, H.L. 2002. Lipopolysaccharide increases resistin gene expression in vivo and in vitro. *FEBS Lett* 530:158-162.

32. Milan, G., Granzotto, M., Scarda, A., Calcagno, A., Pagano, C., Federspil, G., and Vettor, R. 2002. Resistin and adiponectin expression in visceral fat of obese rats: effect of weight loss. *Obes Res* 10:1095-1103.

33. Silswal, N., Singh, A.K., Aruna, B., Mukhopadhyay, S., Ghosh, S., and Ehtesham, N.Z. 2005. Human resistin stimulates the pro-inflammatory cytokines TNF-alpha and IL-12 in macrophages by NF-kappaB-dependent pathway. *Biochem Biophys Res Commun* 334:1092-1101.

34. Kosteli, A., Sugaru, E., Haemmerle, G., Martin, J.F., Lei, J., Zechner, R., and Ferrante, A.W., Jr. 2010. Weight loss and lipolysis promote a dynamic immune response in murine adipose tissue. *J Clin Invest* 120:3466-3479.

35. Boden, G., and Shulman, G.I. 2002. Free fatty acids in obesity and type 2 diabetes: defining their role in the development of insulin resistance and beta-cell dysfunction. *Eur J Clin Invest* 32 Suppl 3:14-23.

36. Memon, R.A., Fuller, J., Moser, A.H., Smith, P.J., Feingold, K.R., and Grunfeld, C. 1998. In vivo regulation of acyl-CoA synthetase mRNA and activity by endotoxin and cytokines. *Am J Physiol* 275:E64-72.

37. Yang, J., Kalhan, S.C., and Hanson, R.W. 2009. What is the metabolic role of phosphoenolpyruvate carboxykinase? *J Biol Chem* 284:27025-27029.

38. Nye, C.K., Hanson, R.W., and Kalhan, S.C. 2008. Glyceroneogenesis is the dominant pathway for triglyceride glycerol synthesis in vivo in the rat. *J Biol Chem* 283:27565-27574.

39. Feingold, K.R., Moser, A., Shigenaga, J.K., and Grunfeld, C. 2011. Inflammation inhibits the expression of phosphoenolpyruvate carboxykinase in liver and adipose tissue. *Innate Immun*.

40. Sethi, J.K., and Hotamisligil, G.S. 1999. The role of TNF alpha in adipocyte metabolism. *Semin Cell Dev Biol* 10:19-29.

41. Suganami, T., Tanimoto-Koyama, K., Nishida, J., Itoh, M., Yuan, X., Mizuarai, S., Kotani, H., Yamaoka, S., Miyake, K., Aoe, S., et al. 2007. Role of the Toll-like receptor 4/NF-kappaB pathway in saturated fatty acid-induced inflammatory changes in the interaction between adipocytes and macrophages. *Arterioscler Thromb Vasc Biol* 27:84-91.

42. Kanda, H., Tateya, S., Tamori, Y., Kotani, K., Hiasa, K., Kitazawa, R., Kitazawa, S., Miyachi, H., Maeda, S., Egashira, K., et al. 2006. MCP-1

contributes to macrophage infiltration into adipose tissue, insulin resistance, and hepatic steatosis in obesity. *J Clin Invest* 116:1494-1505.

43. Kamei, N., Tobe, K., Suzuki, R., Ohsugi, M., Watanabe, T., Kubota, N., Ohtsuka-Kowatari, N., Kumagai, K., Sakamoto, K., Kobayashi, M., et al. 2006. Overexpression of monocyte chemoattractant protein-1 in adipose tissues causes macrophage recruitment and insulin resistance. *J Biol Chem* 281:26602-26614.

44. Tateya, S., Tamori, Y., Kawaguchi, T., Kanda, H., and Kasuga, M. 2010. An increase in the circulating concentration of monocyte chemoattractant protein-1 elicits systemic insulin resistance irrespective of adipose tissue inflammation in mice. *Endocrinology* 151:971-979.

45. Mohamed-Ali, V., Goodrick, S., Rawesh, A., Katz, D.R., Miles, J.M., Yudkin, J.S., Klein, S., and Coppack, S.W. 1997. Subcutaneous adipose tissue releases interleukin-6, but not tumor necrosis factor-alpha, in vivo. *Journal of Clinical Endocrinology & Metabolism* 82:4196-4200.

46. Lee, J.Y., Sohn, K.H., Rhee, S.H., and Hwang, D. 2001. Saturated fatty acids, but not unsaturated fatty acids, induce the expression of cyclooxygenase-2 mediated through Toll-like receptor 4. *J Biol Chem* 276:16683-16689.

47. Itoh, M., Suganami, T., Satoh, N., Tanimoto-Koyama, K., Yuan, X., Tanaka, M., Kawano, H., Yano, T., Aoe, S., Takeya, M., et al. 2007. Increased adiponectin secretion by highly purified eicosapentaenoic acid in rodent models of obesity and human obese subjects. *Arterioscler Thromb Vasc Biol* 27:1918-1925.

48. Shi, H., Kokoeva, M.V., Inouye, K., Tzameli, I., Yin, H., and Flier, J.S. 2006. TLR4 links innate immunity and fatty acid-induced insulin resistance. *J Clin Invest* 116:3015-3025.

49. McCall, K.D., Holliday, D., Dickerson, E., Wallace, B., Schwartz, A.L., Schwartz, C., Lewis, C.J., Kohn, L.D., and Schwartz, F.L. 2010. Phenylmethimazole blocks palmitate-mediated induction of inflammatory cytokine pathways in 3T3L1 adipocytes and RAW 264.7 macrophages. *J Endocrinol* 207:343-353.

50. Ichioka, M., Suganami, T., Tsuda, N., Shirakawa, I., Hirata, Y., Satoh-Asahara, N., Shimoda, Y., Tanaka, M., Kim-Saijo, M., Miyamoto, Y., et al. 2011.

Increased expression of macrophage-inducible C-type lectin in adipose tissue of obese mice and humans. *Diabetes* 60:819-826.

51. Yamasaki, S., Saito, T., Ishikawa, E., Sakuma, M., Hara, H., and Ogata, K. 2008. Mincle is an ITAM-coupled activating receptor that senses damaged cells. *Nature Immunology* 9:1179-1188.

52. Cinti, S., Mitchell, G., Barbatelli, G., Murano, I., Ceresi, E., Faloia, E., Wang, S., Fortier, M., Greenberg, A.S., and Obin, M.S. 2005. Adipocyte death defines macrophage localization and function in adipose tissue of obese mice and humans. *J Lipid Res* 46:2347-2355.

53. Hotamisligil, G.S., Shargill, N.S., and Spiegelman, B.M. 1993. Adipose expression of tumor necrosis factor-alpha: direct role in obesity-linked insulin resistance. *Science* 259:87-91.

54. Sartipy, P., and Loskutoff, D.J. 2003. Monocyte chemoattractant protein 1 in obesity and insulin resistance. *Proc Natl Acad Sci U S A* 100:7265-7270.

55. Kershaw, E.E., and Flier, J.S. 2004. Adipose tissue as an endocrine organ. *Journal of Clinical Endocrinology & Metabolism* 89:2548-2556.

56. Lagathu, C., Yvan-Charvet, L., Bastard, J.P., Maachi, M., Quignard-Boulange, A., Capeau, J., and Caron, M. 2006. Long-term treatment with interleukin-1beta induces insulin resistance in murine and human adipocytes. *Diabetologia* 49:2162-2173.

57. Ozcan, U., Cao, Q., Yilmaz, E., Lee, A.H., Iwakoshi, N.N., Ozdelen, E., Tuncman, G., Gorgun, C., Glimcher, L.H., and Hotamisligil, G.S. 2004. Endoplasmic reticulum stress links obesity, insulin action, and type 2 diabetes. *Science* 306:457-461.

58. Hirosumi, J., Tuncman, G., Chang, L., Gorgun, C.Z., Uysal, K.T., Maeda, K., Karin, M., and Hotamisligil, G.S. 2002. A central role for JNK in obesity and insulin resistance. *Nature* 420:333-336.

59. Rath, E., and Haller, D. 2011. Inflammation and cellular stress: a mechanistic link between immune-mediated and metabolically driven pathologies. *Eur J Nutr* 50:219-233.

60. Weston, C.R., and Davis, R.J. 2007. The JNK signal transduction pathway. *Curr Opin Cell Biol* 19:142-149.

61. Hotamisligil, G.S. 2010. Endoplasmic reticulum stress and the inflammatory basis of metabolic disease. *Cell* 140:900-917.

62. Varga, T., Czimmerer, Z., and Nagy, L. 2011. PPARs are a unique set of fatty acid regulated transcription factors controlling both lipid metabolism and inflammation. *Biochim Biophys Acta* 1812:1007-1022.

63. Lehrke, M., and Lazar, M.A. 2005. The many faces of PPARgamma. *Cell* 123:993-999.

64. Tontonoz, P., Hu, E., and Spiegelman, B.M. 1994. Stimulation of adipogenesis in fibroblasts by PPAR gamma 2, a lipid-activated transcription factor. *Cell* 79:1147-1156.

65. Trujillo, M.E., and Scherer, P.E. 2006. Adipose tissue-derived factors: Impact on health and disease. *Endocrine Reviews* 27:762-778.

66. Sharma, A.M., and Staels, B. 2007. Peroxisome proliferator-activated receptor gamma and adipose tissue--understanding obesity-related changes in regulation of lipid and glucose metabolism. *J Clin Endocrinol Metab* 92:386-395.

67. Lipscombe, L.L., Gomes, T., Levesque, L.E., Hux, J.E., Juurlink, D.N., and Alter, D.A. 2007. Thiazolidinediones and cardiovascular outcomes in older patients with diabetes. *JAMA* 298:2634-2643.

68. Odegaard, J.I., Ricardo-Gonzalez, R.R., Goforth, M.H., Morel, C.R., Subramanian, V., Mukundan, L., Red Eagle, A., Vats, D., Brombacher, F., Ferrante, A.W., et al. 2007. Macrophage-specific PPARgamma controls alternative activation and improves insulin resistance. *Nature* 447:1116-1120.

69. Bouhlel, M.A., Derudas, B., Rigamonti, E., Dievart, R., Brozek, J., Haulon, S., Zawadzki, C., Jude, B., Torpier, G., Marx, N., et al. 2007. PPARgamma activation primes human monocytes into alternative M2 macrophages with anti-inflammatory properties. *Cell Metabolism* 6:137-143.

70. Fujisaka, S., Usui, I., Bukhari, A., Ikutani, M., Oya, T., Kanatani, Y., Tsuneyama, K., Nagai, Y., Takatsu, K., Urakaze, M., et al. 2009. Regulatory

mechanisms for adipose tissue M1 and M2 macrophages in diet-induced obese mice. *Diabetes* 58:2574-2582.

71. Lumeng, C.N., Bodzin, J.L., and Saltiel, A.R. 2007. Obesity induces a phenotypic switch in adipose tissue macrophage polarization. *J Clin Invest* 117:175-184.

72. Choi, J.H., Banks, A.S., Estall, J.L., Kajimura, S., Bostrom, P., Laznik, D., Ruas, J.L., Chalmers, M.J., Kamenecka, T.M., Bluher, M., et al. 2010. Anti-diabetic drugs inhibit obesity-linked phosphorylation of PPARgamma by Cdk5. *Nature* 466:451-456.

73. Cox, J., and Mann, M. 2007. Is proteomics the new genomics? *Cell* 130:395-398.

74. Gygi, S.P., Rist, B., Gerber, S.A., Turecek, F., Gelb, M.H., and Aebersold, R. 1999. Quantitative analysis of complex protein mixtures using isotope-coded affinity tags. *Nat Biotechnol* 17:994-999.

75. Mann, M. 2006. Functional and quantitative proteomics using SILAC. *Nat Rev Mol Cell Biol* 7:952-958.

76. Zieske, L.R. 2006. A perspective on the use of iTRAQ (TM) reagent technology for protein complex and profiling studies. *Journal of Experimental Botany* 57:1501-1508.

77. Steen, H., and Mann, M. 2004. The ABC's (and XYZ's) of peptide sequencing. *Nat Rev Mol Cell Biol* 5:699-711.

78. Choudhary, C., and Mann, M. 2010. Decoding signalling networks by mass spectrometry-based proteomics. *Nat Rev Mol Cell Biol* 11:427-439.

79. Ong, S.E., Blagoev, B., Kratchmarova, I., Kristensen, D.B., Steen, H., Pandey, A., and Mann, M. 2002. Stable isotope labeling by amino acids in cell culture, SILAC, as a simple and accurate approach to expression proteomics. *Mol Cell Proteomics* 1:376-386.

80. Geiger, T., Wisniewski, J.R., Cox, J., Zanivan, S., Kruger, M., Ishihama, Y., and Mann, M. 2011. Use of stable isotope labeling by amino acids in cell culture as a spike-in standard in quantitative proteomics. *Nat Protoc* 6:147-157.

81. Geiger, T., Cox, J., Ostasiewicz, P., Wisniewski, J.R., and Mann, M. 2010. Super-SILAC mix for quantitative proteomics of human tumor tissue. *Nat Methods* 7:383-385.

82. Kruger, M., Moser, M., Ussar, S., Thievessen, I., Luber, C.A., Forner, F., Schmidt, S., Zanivan, S., Fassler, R., and Mann, M. 2008. SILAC mouse for quantitative proteomics uncovers kindlin-3 as an essential factor for red blood cell function. *Cell* 134:353-364.

83. Cox, J., and Mann, M. 2008. MaxQuant enables high peptide identification rates, individualized p.p.b.-range mass accuracies and proteome-wide protein quantification. *Nat Biotechnol* 26:1367-1372.

84. Cox, J., Matic, I., Hilger, M., Nagaraj, N., Selbach, M., Olsen, J.V., and Mann, M. 2009. A practical guide to the MaxQuant computational platform for SILAC-based quantitative proteomics. *Nat Protoc* 4:698-705.

85. Green, H., and Meuth, M. 1974. An established pre-adipose cell line and its differentiation in culture. *Cell* 3:127-133.

86. Farmer, S.R. 2006. Transcriptional control of adipocyte formation. *Cell Metabolism* 4:263-273.

87. Raschke, W.C., Baird, S., Ralph, P., and Nakoinz, I. 1978. Functional macrophage cell lines transformed by Abelson leukemia virus. *Cell* 15:261-267.

88. Crouch, S.P., Kozlowski, R., Slater, K.J., and Fletcher, J. 1993. The use of ATP bioluminescence as a measure of cell proliferation and cytotoxicity. *J Immunol Methods* 160:81-88.

89. Livak, K.J., and Schmittgen, T.D. 2001. Analysis of relative gene expression data using real-time quantitative PCR and the 2(T)(-Delta Delta C) method. *Methods* 25:402-408.

90. Kaiser, P., Meierhofer, D., Wang, X., and Huang, L. 2008. Tandem affinity purification combined with mass spectrometry to identify components of protein complexes. *Methods Mol Biol* 439:309-326.

91. Miyake, Y., Ishikawa, E., Ishikawa, T., and Yamasaki, S. 2010. Self and nonself recognition through C-type lectin receptor, Mincle. *Self Nonself* 1:310-313.

92. Matsumoto, M., Tanaka, T., Kaisho, T., Sanjo, H., Copeland, N.G., Gilbert, D.J., Jenkins, N.A., and Akira, S. 1999. A novel LPS-inducible C-type lectin is a transcriptional target of NF-IL6 in macrophages. *J Immunol* 163:5039-5048.

93. Cohen, P. 2002. The origins of protein phosphorylation. *Nat Cell Biol* 4:E127-130.

94. Hotamisligil, G.S., Peraldi, P., Budavari, A., Ellis, R., White, M.F., and Spiegelman, B.M. 1996. IRS-1-mediated inhibition of insulin receptor tyrosine kinase activity in TNF-alpha- and obesity-induced insulin resistance. *Science* 271:665-668.

95. Gao, X., Li, K., Hui, X., Kong, X., Sweeney, G., Wang, Y., Xu, A., Teng, M., Liu, P., and Wu, D. 2011. Carnitine palmitoyltransferase 1A prevents fatty acid-induced adipocyte dysfunction through suppression of c-Jun N-terminal kinase. *Biochem J* 435:723-732.

96. Suganami, T., Yuan, X., Shimoda, Y., Uchio-Yamada, K., Nakagawa, N., Shirakawa, I., Usami, T., Tsukahara, T., Nakayama, K., Miyamoto, Y., et al. 2009. Activating transcription factor 3 constitutes a negative feedback mechanism that attenuates saturated Fatty acid/toll-like receptor 4 signaling and macrophage activation in obese adipose tissue. *Circ Res* 105:25-32.

97. Prieur, X., Roszer, T., and Ricote, M. 2010. Lipotoxicity in macrophages: evidence from diseases associated with the metabolic syndrome. *Biochim Biophys Acta* 1801:327-337.

98. Hara, T., Hirasawa, A., Ichimura, A., Kimura, I., and Tsujimoto, G. 2011. Free fatty acid receptors FFAR1 and GPR120 as novel therapeutic targets for metabolic disorders. *J Pharm Sci* 100:3594-3601.

99. Witze, E.S., Old, W.M., Resing, K.A., and Ahn, N.G. 2007. Mapping protein post-translational modifications with mass spectrometry. *Nat Methods* 4:798-806.

5.2. Table of Figures

5.3. Index of Tables

5.4. Table of Abbreviations

A-MulV	Abselon Leukemia Virus
ACN	Acetonitrile
AcrP30	Adiponectin
acyl-CoA	Acyl-Coenzym A
AdipiQ	Adiponectin
Adipsin	Complement factor D
Aplp2	Amyloid beta (A4) precursor-like protein 2
apM1	Adiponectin
Arg6	$^{13}C_6$-labeled arginine
ATM	Adipose tissue macrophage
ATP	Adenosine-5'-triphosphate

BSA	Bovine serum albumin
C10	Phenylmathimazole
Car3	Carbonic anhydrase
Cd24a	Cluster of differentiation 24 antigen
Cdk5	Cyclin-dependent kinase 5
cDNA	Copied Deoxyribonucleic acid
CEBPβ	CCAAT/enhancer binding protein β
Cidec	cell death-inducing DFFA-like effector c
Clec4e	Mincle
Clecsf9	Mincle
co	Coculture
CoA	Coenzym A
Cox-2	Cyclooxygenase-2
CPT1	Carnitine-O-palmitoyltransferase 1
CPT1A	Carnitine-O-palmitoyltransferase 1
Cyp2f2	Cytochrome P450, family 2, subfamily f, polypeptide 2
Da	Dalton
Ddx17	RNA helicase
DIFe	Deutsches Institut für Ernährunfsforschung
DMEM	Dulbecco's Modified Eagle Medium
DNA	Deoxyribonucleic acid
dNTP	Desoxyribonukleosidtriphosphate
DTT	Dithiothreitol
EDTA	Ethylenediaminetetraacetic acid
EGTA	Ethylene glycol tetraacetic acid
ELISA	Enzyme linked immunosorbent assays
ER	Endoplasmatic reticulum
ESI	Ionized by electrospray
Fabp4	Fatty acid binding protein 4
FABPs	Fatty acid binding proteins
FBS	Fetal bovine serum
FFA	Free fatty acid

FFAR	Free fatty acid receptors
FT	Fourier transformation
Glut4	Glucosetransporter Typ 4
GPR	G-protein coupled receptor
IBMX	3-Isobutyl-1-methylxanthine
ICAT	Isotope-coded affinity tags
IL-1	Interleukin 1
IL-1β	Interleukin 1β
IL-6	Interleukin 6
IPI	International Protein Index
IR	Insulin receptor
IRS	Insulin receptor subtrate
iTRAQ	Isobaric tags for relative and absolute quantitation
JNK	c-Jun N-terminal kinases
LC	Liquid chromatography
LPL	Lipoprotein lipase
LPS	Lipopolysaccharide
LTQ	Linear ion trap
Lys4	$^{2}H_4$-labeled lysine
MAPK	Mitogen-activated protein kinase
MCP-1	Monocyte chemoattractant protein 1
Mincle	Macrophage-inducible C-type lectin
mRNA	Messenger ribonucleic acid
MS	Mass spectrometry
NF-κB	Nuclear factor κB
Nr1d1	Nuclear receptor subfamily 1, group D, member 1
Nr1d2	Nuclear receptor subfamily 1, group D, member 2
Nr3c1	Nuclear receptor subfamily 3, group C, member 1
pal	Palmitate
PBS	Phosphate buffered saline
PCR	Polymerase chain reaction
Peg10	Retrotransposon-derived protein

PEP	Phosphoenolpyruvate
PEPCK	Phosphoenolpyruvate carboxykinase
PPARγ	Peroxisome proliferator-activated receptor γ
qPCR	Real-time polymerase chain reaction
Rarres2	Retinoic acid receptor responder protein 2
RNA	Ribonucleic acid
RNS	Ribonucleinsäure
RPLC	Reverse phase liquid chromotagraphy
RXR	Retinoic X receptor
Rybp	RING1 and YY1-binding protein
S.D.	Standard deviation
SAP130	Histone deacetylase complex subunit 130
SDS	Sodium dodecyl sulfate
Selenbp1	Selenium-binding protein 1
Ser	Serine
SILAC	Stable isotope labeling with amino acids in cell culture
TBS	Tris buffered saline
TCA	Trichloroacetic acid
TG	Triglyceride
TLR	Toll-like receptor
TLR2	Toll-like receptor 2
TLR4	Toll-like receptor 4
TNFR	Tnfα receptor
Tnfα	Tumor necrosis factor α
Tris	Trishydroxymethylaminomethane
Tween	Polyoxyethylenesorbitanmonolaurate
Txnip	Thioredoxin interacting protein
TZD	Thiazolidinediones
UEES	Urea, EDTA, EGTA, SDS
UPR	Unfolded protein response
VEGF	Vascular Endothelial Growth Factor (VEGF)

Erklärung

Ich versichere hiermit, dass ich die anliegende Arbeit mit dem Thema:

"Cell Biological Studies on Adipocyte-Macrophage Communication"

selbständig verfasst und keine anderen Hilfsmittel als die angegebenen benutzt habe. Die Stellen, die anderen Werken dem Wortlaut oder dem Sinne nach entnommen sind, habe ich in jedem einzelnen Falle durch Angaben der Quelle, auch der benutzten Sekundärliteratur, als Entlehnung kenntlich gemacht.

Diese Arbeit wird nach Abschluss des Prüfungsverfahrens der Universitätbibliothek Konstanz übergeben und ist durch Einsicht und Ausleihe somit der Öffentlichkeit zugänglich.

Als Urheber der anliegenden Arbeit stimme ich diesem Verfahren

□ zu

□ nicht zu

Konstanz, ……. …….

Unterschrift

Danksagung

Ich möchte mich bei Herrn Dr. S. Sauer und Prof. Dr. M. Scheffner für die hervorragende Betreuung bedanken.

Darüber hinaus, möchte ich der gesamten Arbeitsgruppe danken.

Ein ganz besonderer Dank gilt meiner Familie, für ihre Hilfe und Unterstützung.